AN ABSTRACT OF THE THESIS OF

ROBERT CAMERON HEALD for the degree of MASTER OF SCIENCE

in ATMOSPHERIC SCIENCES presented on 20 April 1978

Title: PARAMETERIZATION OF THE OCEANIC MIXED LAYER FOR USE IN GENERAL CIRCULATION MODELS

Abstract Approved: Redacted for Privacy

The behavior of different parameterizations of mixed layer physics when used in an oceanic general circulation model (OGCM) having coarse resolution of the upper ocean is examined. The method of parameterization is expected to have an important effect on the resulting sea surface temperature, and hence affect the model's overall fidelity from the viewpoint of air-sea interaction. Tests of three possible parameterizations differ in the manner in which the mixed layer depth is determined: predetermination, diagnostic determination, or prognostic determination. The sea surface temperature is taken to be equivalent to the top OGCM layer temperature in the first two methods, while it is found prognostically in the third method. Results show that for typical forcing cases such as strong insolation, weak surface cooling or weak winds, mixing is insufficient to cause heat transfer between the top two OGCM layers, which occupy the uppermost 500 m of the model. The predetermined and diagnostically determined mixed layer depth parameterizations reduce to a diffusive mixing parameterization, while the prognostic approach satisfactorily models mixed layer depths for all forcing cases. The prognostic method also agrees most closely with the results of a mixed layer model and with observations.

Parameterization of the Oceanic Mixed Layer for Use in General Circulation Models

by

Robert Cameron Heald

A THESIS

submitted to

Oregon State University

in partial fulfillment of
the requirements for the
degree of

Master of Science

Commencement June 1978

APPROVED:

Redacted for Privacy

Assistant Professor of Atmospheric Sciences
in charge of major

Redacted for Privacy

Chairman of Department of Atmospheric Sciences

Redacted for Privacy

Dean of Graduate School

Date thesis is presented 20 April 1978

Typed by Janice Christensen for Robert Cameron Heald

ACKNOWLEDGMENT

I would like to express my thanks to Dr. Jeong-Woo Kim, my major professor, for his guidance in carrying out this research. Dr. W. Lawrence Gates and Dr. William Quinn also offered valuable insight in this work. Helpful comments were provided by Dr. Larry J. Mahrt, Dr. Ernest W. Peterson and graduate student Chang-Chun Su.

The research leading to this thesis is part of research being conducted by the Oregon State University Climatic Research Institute. This research was supported by the National Science Foundation under Grant No. OCE76-80182.

TABLE OF CONTENTS

LIST OF TABLES

LIST OF FIGURES

LIST OF SYMBOLS

α	Thermal expansion coefficient of sea water
B	Combined long wave, sensible and latent heat fluxes from the ocean surface (back flux); reckoned positive upward
$\hat{B}$	$B/\rho C$
ΔB	Typical fluctuation of B
β	Extinction coefficient of insolation in sea water
C	Specific heat of sea water
c_m	Root-mean-square of turbulent velocity fluctuations
D_b	Background turbulent kinetic energy dissipation
D_c	Dissipation of convective produced turbulent kinetic energy
D_*	Dissipation of wind produced turbulent kinetic energy
ε_m	Parameter relating D_b to h
F_z	Total heat flux through depth z (reckoned positive upward)
$\hat{F}_z$	$F_z/\rho C$
G_*	Wind production of turbulent kinetic energy
g	Gravity
γ	Parameter in the equation for D_*
h	Mixed layer depth
$\hat{h}$	Thickness of the "hat" layer
h_{max}	Daily maximum of the mixed layer depth
J	The number of the bottommost OGCM layer undergoing convective adjustment
k	Index for numbering OGCM layers from top to bottom
κ	Thermal diffusivity
L	The number of the OGCM layer containing the embedded mixed layer base

ℓ	Length scale used to estimate the diffusive time scale of the OGCM
n_G	Parameter in the equation G_*
n_D	Parameter in the equation D_*
p	Fraction of the convectively produced turbulent kinetic energy available for entrainment (penetration factor)
ϕ	General representation of any variable affecting the back flux
Q	Total net heat flux across the ocean surface (reckoned positive downward)
$\hat{Q}_0$	$Q_0/\rho C$
R_z	Insolation at depth z (reckoned positive downward)
$\hat{R}_z$	$R_z/\rho C$
ρ	Density of sea water
T	Temperature
T_{-h}	Temperature just below the mixed layer base
T_k	Temperature of the k-th OGCM layer
$T_{1_{max}}$	Daily maximum temperature of the first (top) OGCM layer
T_m	Mixed layer temperature
$T_{m_{max}}$	Daily maximum mixed layer temperature
$\hat{T}$	Temperature of the "hat" layer
T'	Fluctuation of the temperature due to turbulent motion
ΔT	Temperature jump across the mixed layer base
t	Time
t^*	Period of diurnal cycle of insolation
τ	Time scale of the temperature change of the top OGCM layer due to diffusion
U_s	Surface wind speed

u_*	Friction velocity in the mixed layer
$\overline{w}$	Mean vertical velocity in the ocean
w_e	Rate of increase of the mixed layer depth (entrainment rate)
w'	Fluctuation of the vertical component of velocity due to turbulent motion
z	Depth
z_J	Depth of the base of the J-th OGCM layer
z_k	Depth of the base of the k-th OGCM layer
z_L	Depth of the base of the L-th OGCM layer
Δz_k	Thickness of the k-th OGCM layer

PARAMETERIZATION OF THE OCEANIC MIXED LAYER FOR USE IN GENERAL CIRCULATION MODELS

I. INTRODUCTION

Realization that the sea surface temperature (SST) is an important factor affecting the amount of heat flux between ocean and atmosphere has stimulated research to develop mathematical models of the upper oceanic mixed layer in order to more accurately determine SST. The apparent relationship of large scale SST anomalies to changes in the general circulation of the atmosphere has led to the development of methods for parameterizing the mixed layer for use in oceanic general circulation models (OGCM's). This thesis describes and tests three possible methods of parameterization of mixed layer for use in an OGCM with coarse vertical resolution of the upper ocean.

Two recent papers have suggested possible parameterization methods. The first is Bryan *et al.* (1975), in which the wind mixing considered by Kraus and Turner (1967) is parameterized and heat redistributed downward through successive OGCM layers, so that heat is conserved and the potential energy gained during the mixing is equal to the energy supplied by the wind. The second method, suggested by Haney and Davies (1976), assumes the mixed layer depth to be the lesser of the Ekman depth and the Monin-Obukhov length. They include both wind mixing and convective mixing and obtain the heat flux at the bottom of the mixed layer, from which they compute the heat flux at the base of any OGCM layer within the mixed layer by linear inter-

polation between the values of the heat flux at the top and bottom of the mixed layer.

In an OGCM with arbitrarily many layers to describe the uppermost layers of the ocean, different parameterizations of the mixed layer may produce similar results since the mixed layer depth is always close to the depth of an integer number of OGCM layers. However, as vertical resolution is decreased and fewer OGCM layers are used to describe the mixed layer, various parameterizations may yield significantly different results. It is therefore of interest when examining the behavior of various parameterizations to use an OGCM with coarse vertical resolution of the upper ocean. The model of Bryan *et al.* uses three layers and Haney and Davies' model uses five layers to describe the top 200 meters of the ocean, the depth of which is approximately the lower limit of the mixed layer base. The OGCM used here contains only two layers to describe the uppermost 500 meters and thus is expected to produce significantly different results depending on the parameterization method used.

The three methods chosen differ primarily in the manner in which the mixed layer depth is obtained. In the first method the mixed layer depth is the depth of the base of one or more OGCM layers (50, 500, 2500, or 5000 m). In the second method the mixed layer depth is found diagnostically in a manner similar to that used by Haney and Davies to obtain the Monin-Obukhov length, and in the third it is determined prognostically as was done by Kim (1976). In view of the prognostic determination of the mixed layer depth, the mixed layer

temperature is explicitly predicted to give the SST in the prognostic method, whereas the SST is equated to the temperature of the uppermost OGCM layer in the methods in which the mixed layer depth is either predetermined or determined diagnostically.

Chapter II contains a brief description of the factors influencing the evolution of the upper oceanic mixed layer, a review of previous models of the mixed layer, and a description of the model to be parameterized and embedded into the OGCM. The three parameterization methods to be considered are described in Chapter III and the results of the experimental runs are described in Chapter IV. Chapter V contains further discussion and suggestions for possible improvement of the parameterization methods.

II. THE UPPER OCEANIC MIXED LAYER

The vertical structure of the upper oceanic mixed layer is quite uniform, due to active turbulent mixing which destroys gradients of momentum, temperature and salinity (see figure 1).

Variations in the depth of the mixed layer depend on the relative importance of insolation, surface heat loss (back flux) and surface wind speed. The absorption of penetrative insolation decreases with depth so that it acts to stratify the upper layers of ocean. Turbulent kinetic energy generated by the back flux and wind act to destroy this stratification. This back flux cools the ocean surface, generating cold plumes which sink and create convective motions; wind stress generates turbulence by creating shear within the mixed layer. If the turbulent kinetic energy generated by either the back flux or wind is insufficient to balance dissipation by friction, and stratification due to insolation, the mixed layer will become shallower. If excess energy is available some of it will be converted to potential energy as colder, denser water below the mixed layer is replaced by turbulent warmer mixed layer water through the mechanism of entrainment. Entrainment results in deepening of the mixed layer as the interface separating turbulent and quiescent water moves downward. Some of the excess energy is also used to generate the turbulent motions of the newly entrained quiescent water (spin up). The rate of mixed layer deepening is given by

$$\frac{\partial h}{\partial t} = w_e - \overline{w}$$

(for definitions of these and other symbols to be introduced later refer to the List of Symbols).

Variations of the temperature of the mixed layer are due to the net heat flux into the layer by insolation, back flux and entrainment:

$$\frac{\partial T_m}{\partial t} = \frac{(\hat{R}_0 - \hat{R}_{-h} - \hat{B}) + (\overline{w'T'})_{-h}}{h} \quad . \qquad (1)$$

The depth of the mixed layer fluctuates from tens to hundreds of meters over a wide range of time scales from hours to months in response to variations in insolation, back flux and surface wind speed. Insolation varies primarily on diurnal, synoptic and annual time scales. During the day, the mixed layer tends to become shallower because of the dominant influence of insolation; at night the layer becomes deeper when excess energy is available causing entrainment to occur. Diurnal variation of the mixed layer depth and temperature is the result. On the annual scale varying solar declination causes variation of the daily mean insolation. This variation is responsible for the annual cycle of the mixed layer depth and temperature. Variations of surface wind, cloud cover, and surface air temperature and humidity influence the evolution of the mixed layer on a wide range of time scales, including those already mentioned, by regulating the surface fluxes of momentum and heat.

Besides solar and atmospheric influences, the thermal structure of the water below the mixed layer, the thermocline, affects the rate of deepening of the mixed layer. The thermal structure of the daily thermocline is the past history of the mixed layer temperature and is

formed during periods of shallowing on diurnal scales. The daily thermocline, however, is diurnally eroded as the mixed layer deepens nightly to the depth of the seasonal thermocline, which is similarly the past history of the mixed layer temperature and is formed during periods of shallowing on an annual scale. The seasonal thermocline is annually eroded as the mixed layer deepens in cold seasons and eventually reaches the depth of the permanent thermocline.

Large scale ocean structure can also influence mixed layer evolution. Horizontal advections of oceanic properties such as SST or mixed layer depth may influence the evolution of the mixed layer locally.

Several one dimensional models of the upper mixed layer have been developed in recent years. Kitaigorodsky (1960) found the summer mixed layer depth diagnostically by balancing the opposing effects of insolation and wind stress. Kraus and Rooth (1961) considered the absorption of insolation at depth and pointed out the possibility of convective production of turbulent energy. Kraus and Turner (1967) then developed a time dependent model of the seasonal thermocline including both wind and convective mixing, but neglecting the dissipation of turbulent energy; shallowing of the mixed layer in response to increased insolation during the spring and summer months generated a seasonal thermocline which was subsequently eroded during deepening in colder months. Denman (1973) considered diurnal and synoptic scale forcing of the mixed layer, and included an energy dissipation which was proportional to the surface wind stress. Pollard *et al.* (1973)

considered the effects of turbulence and resultant entrainment due to the inertial shear near the bottom of the mixed layer.

Alexander and Kim (1976) found that the Kraus-Turner diagnostic model for mixed layer depth, which was an extension of the Kitaigorodsky model, gave realistic results for the summer North Pacific Ocean, provided the effect of dissipation was appropriately included to limit mixed layer depths, particularly in regions where heating was weak. The dissipation consisted of a wind dissipation and a background dissipation; the wind dissipation D_* varied exponentially with mixed layer depth according to

$$D_* = n_D \rho u_*^3 (1 - e^{-\gamma h}) \tag{2}$$

where u_* depends on the wind stress (see for examples Denman, 1973). The background dissipation D_b varied linearly with h according to $D_b = \rho \varepsilon_m h$. Kim (1976) used the dissipation scheme of Alexander and Kim (1976) in a prognostic mixed layer model, choosing $\gamma \to \infty$ so that D_* remained constant with changes in mixed layer depth. He also incorporated a storage term which allowed prognostic determination of the mixed layer depth in the shallowing case.

The mixed layer model to be used in the parameterization methods is a modification of the one dimensional model of Kim (1976) (see figures 2 and 3). The equations describing the mixed layer (see for example Kim, 1976) are

$$(\overline{w'T'})_{-h} = -\hat{B} + \hat{R}_0 + \hat{R}_{-h} - \frac{2}{h}\int_{-h}^{0}\hat{R}_z dz + \frac{2}{h}\int_{-h}^{0}\overline{w'T'}dz \qquad (3)$$

$$\tfrac{1}{2}\rho c_m^2 w_e = G_* - D_* - D_b + \rho g\alpha\int_{-h}^{0}\overline{w'T'}dz \qquad (4)$$

$$(\overline{w'T'})_{-h} = -w_e\Delta T \quad . \qquad (5)$$

Equation (3) states that the total heat flux varies linearly over the depth of the mixed layer, and is based on the assumption that changes in temperature occur uniformly over the depth of the layer. Equation (4) expresses the conservation of energy in the mixed layer. The entrainment rate is now equivalent to the time rate of change of the mixed layer depth

$$w_e = \frac{\partial h}{\partial t}$$

since $\overline{w}$ is taken as zero in a one dimensional model. Equation (5), the jump equation, states that the vertical heat flux is continuous across the interface between the turbulent mixed layer and the quiescent water just below it, where

$$\Delta T = T_m - T_{-h} \qquad (6)$$

(see figure 2). Combining (3), (4) and (5) gives the entrainment rate

$$w_e = \frac{\hat{B} - \hat{R}_0 - \hat{R}_{-h} + \frac{2}{h}\int_{-h}^{0}\hat{R}_z dz + \frac{2}{\rho g\alpha h}(G_* - D_* - D_b)}{\Delta T + \frac{c_m^2}{g\alpha h}} \quad . \qquad (7)$$

Two modifications to the model of Kim (1976) are made. The first modification is the replacement of the background dissipation by a con-

vective dissipation. The back flux B accounts for the entrainment due to the formation of cold plumes which penetrate the mixed layer base. Gill and Turner (1976) suggested that only a small part of the energy generated by formation of cold plumes acts to entrain while the rest is lost to dissipation. Thus a better estimate of the effect of surface cooling would be to replace B with pB where p has a value between zero and one. This is equivalent to replacing the background dissipation in (7) with a convective energy dissipation D_c:

$$w_e = \frac{\hat{B} - \hat{R}_0 - \hat{R}_{-h} + \frac{2}{h}\int_{-h}^{0} \hat{R}_z dz + \frac{2}{\rho g \alpha h}(G_* - D_* - D_c)}{\Delta T + \frac{c_m^2}{g\alpha h}} \tag{8}$$

where

$$D_c = \tfrac{1}{2}\rho g \alpha h \,(1 - p)\hat{B} \quad . \tag{9}$$

The other modification concerns the values assigned to n_D and n_G, the latter being the parameter in the equation for the wind production of turbulent energy:

$$G_* = n_G \rho u_*^3 \tag{10}$$

(see for example Kim, 1976). If buoyancy effects within the mixed layer are absent the energy available for entrainment is

$$G_* - D_* = n_G \rho u_*^3 - n_D \rho u_*^3 (1 - e^{-\gamma h}) \quad .$$

The parameter n_G can be found in terms of n_D by letting $h \to \infty$. Then $G_* - D_* = (n_G - n_D)\rho u_*^3 = 0$ and therefore $n_G = n_D$ since for very large h the wind produced energy should be completely dissipated. Kantha

et al. (1977) found n_D by measuring w_e in a laboratory model. In the model, buoyancy within the mixed layer was not present (R = B = 0) so that (8) can be written as

$$\tfrac{1}{2}(1 + Ri)\rho c_m^2 w_e = G_* - D_* = n_D \rho u_*^3 e^{-\gamma h} \tag{11}$$

where

$$Ri \equiv \frac{g\alpha h \Delta T}{c_m^2} \quad .$$

In addition the experimental conditions were such that Ri >> 1 and $\gamma h << 1$ so that (11) becomes

$$\frac{w_e}{u_*} = \frac{2u_*^2}{c_m^2 Ri}\, n_D$$

or

$$\frac{w_e}{u_*} = \frac{2}{Ri^*}\, n_D$$

where

$$Ri^* \equiv \frac{c_m^2}{u_*^2}\, Ri \quad .$$

Kantha *et al.* (1977) measured w_e/u_* under the above conditions for various Ri* and obtained a value for n_D of 3.0. The values $n_G = n_D = 3.0$ are used here in place of those used by Kim (1976).

By combining (2), (8) and (10), using (9) in place of D_b, and letting $n \equiv n_G = n_D$, the entrainment rate becomes

$$w_e = \frac{p\hat{B} - \hat{R}_0 \left[1 - \frac{2}{\beta h} + e^{-\beta h}\left(1 + \frac{2}{\beta h}\right) \right] + \frac{2nu_*^3 e^{-\gamma h}}{g\alpha h}}{\Delta T + c_m^2/g\alpha h} \tag{12}$$

where the insolation is assumed to decrease exponentially with depth

$$\hat{R}_z = \hat{R}_0 e^{\beta z} \quad . \tag{13}$$

III. THE METHODS OF PARAMETERIZATION OF THE MIXED LAYER

The modified model of Kim (1976) described above (hereafter called KIM) may be parameterized in various ways so that it can be embedded into an OGCM to provide a more physically realistic value of the SST. Three parameterization methods have been chosen which differ in the manner in which the mixed layer depth is determined, as noted previously (see Table 1).

The OGCM is a one dimensional version of the coarse vertical resolution model of Kim and Gates (1978) (see figure 4). The model contains four layers with thicknesses from top to bottom of 50, 450, 2000, and 2500 meters which are designated Δz_1, Δz_2, Δz_3 and Δz_4 respectively. Heat is exchanged by diffusion between any two consequent layers in proportion to the temperature gradient between them; in addition the uppermost layer also responds to the net heat input at the sea surface. The heat flux, $F_{k+\frac{1}{2}}$, between the k-th and (k+1)-th layers is

$$\begin{aligned} \hat{F}_{k+\frac{1}{2}}(t) &= -\kappa \frac{T_k - T_{k+1}}{\frac{1}{2}(\Delta z_k + \Delta z_{k+1})} , \quad k = 1,2,3 \\ &= -\hat{Q} \quad , \quad k = 0 \\ &= 0 \quad , \quad k = 4 \end{aligned} \tag{14}$$

where $Q_0 \equiv R_0 - B$. The insolation reaching $-\Delta z_1$ is so small that it may be neglected, i.e. $R_{-\Delta z_1} = 0$. The change of temperature of any OGCM layer depends on the net heat flux into that layer:

$$T_k(t + \Delta t) = T_k(t) - \frac{\hat{F}_{k-\frac{1}{2}}(t) - \hat{F}_{k+\frac{1}{2}}(t)}{\Delta z_k} \Delta t, \quad k = 1,2,3,4 \quad . \qquad (15)$$

Should (15) predict $T_k(t + \Delta t) < T_{k+1}(t + \Delta t)$, the two temperatures are reset to their depth-weighted average temperature so that the total heat content is conserved (hereafter referred to as convective adjustment). For the purpose of comparison, the OGCM without an embedded mixed layer will be included in the runs of the three mixed layer parameterization methods to be described next.

The Predetermined Mixed Layer Depth Method (CONS)

The simplest of the three parameterization methods predetermines the mixed layer depth as the depth of the base of one or more OGCM layers previously undergoing convective adjustment. Convective adjustment will have occurred if $T_k < T_{k+1}$ in the same manner as described with respect to DIFF. For example, the mixed layer depth increases to $h = \Delta z_1 + \Delta z_2$ if convective adjustment between only the top two OGCM layers has occurred. In general

$$h = z_J \equiv \sum_{k=1}^{J} \Delta z_k$$

In this parameterization the turbulent kinetic energy in the mixed layer is assumed to be constant so that the storage term on the left-hand side of (4) is zero giving

$$0 = G_* - D_* - D_c + \rho g \alpha \int_{-h}^{0} \overline{w'T'} \, dz$$

with D_c again replacing D_b.

Combining this equation with (2), (3), and (13) gives the heat flux due to entrainment

$$(\overline{w'T'})_{-h} = -p\hat{B} + \hat{R}_0 + \hat{R}_{-h} - \frac{2\hat{R}_0}{\beta h}(1-e^{-\beta h}) - \frac{2nu_*^3 e^{-\gamma h}}{g\alpha h} \quad . \qquad (16)$$

The total flux through the base of the J-th layer $F_{J+\frac{1}{2}}$ is then

$$\hat{F}_{J+\frac{1}{2}}(t) \equiv (\overline{w'T'})_{-z_J} = -p\hat{B} + \hat{R}_0 - \frac{2\hat{R}_0}{\beta z_J}(1-e^{-\beta z_J}) - \frac{2nu_*^3 e^{-\gamma z_J}}{g\alpha z_J} \qquad (17)$$

where the insolation at the mixed layer base R_{-z_J} is again neglected. When insufficient energy is available for mixing, (17) gives an unrealistic positive value indicating upward heat flux into the mixed layer; in this case (14) is used with Δz_k replaced by z_J to obtain the heat flux. In other words, if a downward heat flux (entrainment) does not occur at $-z_J$ the model behaves exactly like DIFF. The OGCM layer temperature can be found using (15), however in the case of convective adjustment the temperature T_J of the layer z_J is given by

$$T_J(t + \Delta t) = T_J(t) + \frac{\hat{Q}_0(t) + \hat{F}_{J+\frac{1}{2}}(t)}{z_J}\Delta t \quad .$$

The temperature of the top layer T_1 represents the SST in this parameterization.

The Diagnostic Mixed Layer Depth Method (DIAG)

The second parameterization method finds the mixed layer depth diagnostically. As in CONS the turbulent kinetic energy is assumed to be constant. In addition the mixed layer is assumed to have reached an equilibrium in which wind and convective mixing energeti-

cally balance dissipation, so that neither entrainment nor shallowing is occurring. Equation (16) under such equilibrium becomes

$$0 = p\hat{B} - \hat{R}_0 \left[1 - \frac{2}{\beta h} + e^{-\beta h}\left(1 + \frac{2}{\beta h}\right) \right] + \frac{2nu_*^3 e^{-\gamma h}}{g\alpha h} \qquad (18)$$

and can be solved for h using Newton's method.

Figure 5 shows two examples of $(\overline{w'T'})_{-h}$ as a function of h from (16). Note that as $R \to pB$, the equilibrium mixed layer depth as described above becomes very large. Thus (18) cannot be used to find h when $R \leq pB$ because $(\overline{w'T'})_{-h} \leq 0$ for all positive h. If this occurs then the heat flux between layers of the OGCM is again found using (14). If $R > pB$, however, the flux at any interface within the mixed layer can be found by linear interpolation of the fluxes at the mixed layer base and at the sea surface. At the mixed layer base the total flux is $F_{-h} = -R_{-h}$ since $(w'T')_{-h} = 0$; at the sea surface $F_{\frac{1}{2}} = -Q_0$. By interpolation the fluxes at layer interfaces within the mixed layer are

$$\hat{F}_{k+1} = (\overline{w'T'})_{-z_k} - \hat{R}_{-z_k} = (\hat{Q}_0 - \hat{R}_{-h}) z_k/h - \hat{Q}_0$$

where z_k is the depth of the base of the k-th layer. The fluxes through layer interfaces below the mixed layer base continue to be given by (14). Thus for the case of $h < \Delta z_1$ all interfacial fluxes are found by (14) and the results are identical to the results using DIFF. The OGCM layer temperatures T_k are given by (15) and the uppermost layer temperature is chosen to represent the SST.

The Prognostic Mixed-Layer Depth Method (PROG)

The third parameterization method uses the prognostic equation for the mixed layer depth:

$$h(t + \Delta t) = h(t) + w_e \Delta t \quad .$$

If the initial mixed layer depth is known at time t it can be found at a time $t + \Delta t$ by knowing the entrainment rate w_e during this time interval. If T_{-h} in (6) is known w_e can be found using (12). In mixed layer models such as that of Denman (1973) or Kim (1976) T_{-h} is known because details of the thermocline structure are retained (see figure 3). However, in an embedded model T_{-h} must be estimated since an explicit record of the thermocline structure is not available. The method used to estimate T_{-h} is a weighted average of T_m and $\hat{T}$, where $\hat{T}$ is defined as

$$\hat{T} \equiv \frac{\sum_{k=1}^{L} T_k \Delta z_k - T_m h}{\hat{h}} \tag{19}$$

and the "hat" layer $\hat{h}$ is

$$\hat{h} \equiv \sum_{k=1}^{L} \Delta z_k - h$$

(see figure 6). The equation for estimating T_{-h} is

$$T_{-h} = \frac{\hat{T} - T_{L+\frac{1}{2}}}{T_L - T_{L+\frac{1}{2}}} T_m + \frac{T_L - \hat{T}}{T_L - T_{L+\frac{1}{2}}} \hat{T} \tag{20}$$

where

$$T_{L+\frac{1}{2}} \equiv \frac{T_L + T_{L+1}}{2} \quad , \; L = 1,2,3 \qquad (21)$$

$$\equiv T_L \quad , \; L = 4 \quad .$$

The value of $\hat{T}$ is restricted to values greater than $T_{L+\frac{1}{2}}$. Figure 7 shows T_{-h} as a function of $\hat{T}$ and includes three other simple schemes for estimating T_{-h} for comparison.

The mixed layer temperature can also be found prognostically once the current mixed layer depth is known. Using (1) and (5) the time rate of change of T_m becomes

$$\frac{dT_m}{dt} = \frac{Q_0 - R_{-h} - w_e \Delta T}{h}$$

where the assumption of horizontal uniformity in a one dimensional model allows the use of the total time derivative. The independently determined T_m represents the SST. If $h > \Delta z$ the top OGCM layer is completely within the mixed layer and T_1 must equal T_m; if they are different T_1 is reset to T_m. Similarly, for deeper mixed layers containing two or more OGCM layers, all layers completely within the mixed layer are reset to T_m. To conserve heat in the OGCM, T_L is then adjusted to a new value of T_L' to compensate for the adjustment of T_1, $\ldots, T_{L-1}$ according to

$$T_L' = T_L + \left[\sum_{k=1}^{L-1} T_k \Delta z_k - T_m \sum_{k=1}^{L-1} \Delta z_k \right] / z_L \quad .$$

As in the other parameterizations, if $T_k < T_{k+1}$ convective adjustment resets the two OGCM temperatures to their depth-weighted average tem-

perature. In addition, if T_m is found to be less than $\hat{T}$ an unstable condition is assumed and T_m and $\hat{T}$ are adjusted to their depth-weighted average temperature and the mixed layer depth is extended down to the base of the L-th layer.

IV. EXPERIMENTAL RUNS WITH THE METHODS

The experimental runs were designed to investigate the characteristic behavior of SST and mixed layer depth of each parameterization method in response to diurnal and synoptic scale forcing, when the forcing was such that the mixed layer processes were confined to the uppermost OGCM layer.

Technical information regarding the computational methods used in these runs is described by Kim and Heald (1978).

Six experimental runs of each of the three parameterizations (CONS, DIAG, and PROG) were made (see Table II). The first five runs (T1, T2, T3, D1 and D2) used hypothetical boundary and initial conditions. Some runs were chosen to exhibit behavior in response to wind forcing while others were designed to study convective processes. The mixed layer model (KIM) was also used for these runs in order to have a standard by which to compare the results of the parameterization methods. The sixth run (DM) was made to compare the parameterization methods with actual observations. The observations used were for a two week long period in June 1970 at Ocean Station PAPA (30N,140W) (Denman and Miyake, 1973). The values of the parameters γ, β, p and κ are those suggested by Kim (personal communication) and are given in Table III.

The duration of the five hypothetical runs was five days. This duration was used so that repeating diurnal variation and longer time scale transient behavior could be recognized. The runs were designed to have zero net daily heat input, so that changes in daily average

OGCM layer temperatures would be due only to redistribution of heat between layers of the model (see Table III).

All the hypothetical runs used the same initial conditions of temperature and mixed layer depth. The initial temperatures of the OGCM layers were chosen to eliminate the possibility of convective adjustment of T_k. Thus in CONS J = 1 at all times.

The first three runs were designed to study the behavior of the parameterization methods if the insolation were constant. In this case $R_0 = \overline{R}_0$ where $\overline{R}_0$ is the daily average insolation. The insolation is balanced by the back flux (R_0 = B) so that the net heat flux into the OGCM is zero for each individual time step.

Convective Mixing with Constant Insolation (Run T1)

In the first run (T1) the response of parameterization methods to only convective processes is examined. The insolation and back flux are given constant values of 300 ly day^{-1} while the surface wind speed U_s is zero in order to eliminate wind mixing.

Both CONS and DIAG (figure 8 and 9) computed an upward heat flux at $-\Delta z_1$, so that (14) was used in these cases and the temperature T_1 was identical to that obtained using DIFF (figure 8). The rate of increase in T_1 is proportional to $T_1 - T_2$, and has a time scale which may be estimated from $\tau \sim \ell^2/\kappa$ where $\ell = (\Delta z_1 + \Delta z_2)/2$. This gives a value of 6.25×10^8 s or about 20 years so that changes in T_1 due strictly to diffusion occur very slowly.

The insufficient mixing energy which caused an upward heat flux

in CONS and DIAG resulted in shallowing of the mixed layer in PROG (figure 10). At a mixed layer depth of 50 meters $w_e = 2.62 \times 10^{-3}$m s^{-1}. The mixed layer temperature T_m cooled at a rate of 2.9×10^{-6}C day^{-1} due to the net heat loss by transmission of insolation R_{-h} through the mixed layer base. Diffusion caused T_1 to decrease at the rate of 7.0×10^{-4}C day^{-1}. As the mixed layer shallowed R_{-h} increased until $dT_m/dt = -8.2 \times 10^{-4}$C day^{-1} when h was 25 m. Further cooling as the mixed layer continued to shallow caused T_m to become less than T_1. This is an unstable condition since $\hat{T}$ must then be greater than T_m; convective adjustment within the top OGCM layer then resulted in $T_m \rightarrow \hat{T} \rightarrow T_1$ and $h \rightarrow \Delta z_1$. As T_1 and T_m continued to cool the process repeated itself with a cycle of five time steps. During each cycle $T_m - T_1$ reach a maximum of about .0001 C. This short term variation of T_m was superimposed on the long time scale diffusive cooling of T_1.

Wind Mixing (Run T2)

In run T2 the influence of only wind stress is investigated using a value of 7.5 m s^{-1} for U_s. The fluxes R_0 and B are zero in order to eliminate buoyancy effects within the mixed layer.

Without the stratifying influence of insolation the downward heat flux at $-\Delta z_1$ using CONS (figure 12) was

$$\hat{F}_{1\frac{1}{2}} = \frac{2nu_*^3 e^{-\gamma \Delta z_1}}{g\alpha \Delta z_1} \quad ,$$

where z_J has been replaced by Δz_1 in (17). This flux replaced the diffusion mechanism and resulted in a linear decrease in T_1. Since

R_0 and B were zero in this run, (18) could not be used to find h in DIAG (figure 13); wind mixing was replaced by diffusion and the temperatures were equivalent to those obtained using DIFF (figure 8).

The results using PROG (figure 14) exhibited a nonlinear entrainment rate. Note that the entrainment rate using KIM (figure 15) was much less but dT_m/dt was larger. This can be explained by the fact that the heat flux due to entrainment $-w_e\Delta T$ was larger in KIM. The heat flux may be found by multiplying both sides of (12) by $-\Delta T$:

$$-w_e\Delta T = \frac{-p\hat{B} + \hat{R}_0\left[1 - \frac{2}{\beta h} + e^{-\beta h}\left(1 + \frac{2}{\beta h}\right)\right] - \frac{2nu_*^3 e^{-\gamma h}}{g\alpha h}}{1 + c_m^2/g\alpha h\Delta T} \quad . \qquad (22)$$

With a mixed layer depth of about 52 m, ΔT was about 1 C using KIM, so that the second term in the denominator of (22) was $\mathcal{O}(10^{-2})$. Using PROG the value of ΔT was about 10^{-2}C so that the second term in the denominator of (22) was $\mathcal{O}(1)$, and the heat flux was therefore considerably less than the flux obtained using KIM.

Wind and Convective Mixing with Constant Insolation (Run T3)

In run T3 the combined effect of both convective and wind mixing are examined. The boundary conditions used are $R_0 = B = 300$ ly day^{-1} and $U_s = 7.5$ m s^{-1}.

Insolation inhibited the entrainment caused by wind and convective mixing so that in CONS (figure 8) and DIAG (figure 16) insufficient energy was available to cause entrainment $-\Delta z_1$, and T_1 was again identical to that obtained from DIFF (figure 8) in both cases.

Using PROG (figure 17) the mixed layer depth shallowed rapidly to a depth of about 32 meters, the approximate diagnostic mixed layer depth found by DIAG. The time scale of the transition from the initial depth to the diagnostic depth was of the order of a few hours. At the diagnostic mixed layer depth the transmitted insolation was quite small and T_m cooled more slowly than T_1 (2.4×10^{-4}C day^{-1} for T_m versus 7.0×10^{-4}C day^{-1} for T_1), so that convective adjustment never occurred as it did in run T1.

Convective Mixing with Variable Insolation (Run D1)

Whereas the transient runs were designed to show transient responses of the parameterizations to various constant forcing regimes, the diurnal runs (D1 and D2) were designed to show the response of the parameterizations to diurnally varying insolation. The insolation for runs D1 and D2 is given by

$$R_0 = -\bar{R}_0 \pi \cos\left(\frac{2\pi t}{t^*}\right) \quad \text{day}$$

$$= 0 \quad \text{night}$$

where t = 0 at midnight. In both runs D1 and D2 300 ly day^{-1} is used for $\bar{R}_0$ and B so changes in T_k from one day to the next are due only to redistribution of heat within the OGCM.

In run D1, U_s is set to zero so that only the effects of convective mixing may be studied as was done in run T1.

Using CONS (figure 19), diffusion occurred as heating during the day prohibited entrainment at $-\Delta z_1$, and the results were similar to

those obtained using DIFF (figure 18). However, at night entrainment occurred due to convective mixing ($F_{1\frac{1}{2}} = -pB$), and T_1 cooled more rapidly than it did using DIFF. For the period when $R > pB$, h was less than Δz_1 so that the results using DIAG (figure 20) were equivalent to those using DIFF for the entire run.

Mixing which was limited to the mixed layer depth in PROG (figure 21) caused significantly greater warming during the day than was obtained using either CONS or DIAG. The mixed layer depth approached the diagnostic value during shallowing as it did in run T3 but the insolation changed too rapidly for h to reach equilibrium. At night cooling of the mixed layer began but entrainment was small due to the absence of wind mixing. This caused strong cooling of T_m until it was less than T_1 so that convective adjustment occurred. In contrast, when T_m cooled sufficiently using KIM (figure 22), convective overturning resulted in the mixed layer deepening by only an amount Δh (see figure 3). However, since PROG does not retain the sub-mixed layer structure, convective adjustment can only occur when $T_m < \hat{T}$. After h deepened to $-\Delta z_1$, using PROG, convective penetration into the second OGCM layer caused cooling of T_m and T_1 and warming of T_2.

Wind and Convective Mixing with Variable Insolation (Run D2)

In this run the effect of wind on a diurnally varying mixed layer is included. The wind speed is 7.5 m s^{-1} and $\bar{R}_0$ and B are, as in run D1, 300 ly day^{-1}.

Using CONS (figure 23) the addition of wind mixing increased the

entrainment rate during the night, although the results showed it to be absent and replaced by diffusion during the day. Using DIAG (figure 24) the mixed layer grew to a greater depth than in run D1, but still fell short of $-\Delta z_1$, so that T_1 was again identical to that obtained using DIFF (figure 18).

Using PROG (figure 25) the mixed layer did not shallow as much as in run D1 because of the additional energy supplied by the wind. At night wind mixing generated enough entrainment to prevent the rapid cooling found in run D1. Since PROG does not retain a sub-mixed layer history during shallowing, the deepening phase resulted in a warmer, shallower mixed layer at the end of the deepening cycle than existed one day earlier. A new period of shallowing and warming built on the existing state to further warm the layer. The daily minimum depth (h_{min}) was the same each day because during shallowing the mixed layer depth approached the diagnostic value on a time scale of the order of a few hours. However, the time scale of the daily maximum of h (h_{max}) was much longer and was related to the rate of entrainment. Since h_{min} was constant, the remaining variable initial condition before deepening occurred (ignoring slow changes in T_1 and T_2) was the daily maximum of T_m (T_{max}). Each day as T_m became warmer, $\hat{T}$ became correspondingly cooler. The results show that ΔT then increased. With h equal to h_{min}, ΔT was initially 0.0014 C and then increased toward a limiting value of about 0.013 C several days later. This reduced the rate of entrainment so that h_{max} decreased each succeeding day.

Two 90-day runs were made using PROG in order to determine the extent of the changes in $T_{m_{max}}$ and h_{max}. The initial boundary conditions were identical to run D2, except that in the first run κ was zero, so that diffusive mixing would not occur when $h < \Delta z_1$. In the first run the time scale of the change in h_{max} and $T_{m_{max}}$ was about 10 days, reaching approximate values of 40 m and 7.1 C respectively. The tendency of $T_{m_{max}}$ to approach a limiting value can be understood by referring to (22). For $\Delta T = 0.0014$ C the second term in the denominator is $\mathcal{O}(10)$. The entrainment heat flux was therefore dependent on ΔT. Later, as ΔT increased, the heat flux increased and the mixed layer warming was reduced. The second 90-day run used the normal value for κ of 0.0001 $m^2 s^{-1}$. After the transient phase observed in the first run, $T_{m_{max}}$ began to decrease at the same rate as $T_{1_{max}}$ (the daily maximum of T_1) and h_{max} began to slowly increase. The maximum difference observed between $T_{m_{max}}$ and $T_{1_{max}}$ reached about 0.06 C during the initial transient phase. A time series of the midnight values of T_m, T_1 and h from these runs (figures 27 and 28) also shows the behavior characterized by their respective daily maximum values.

Simulation of Observed Mixed Layer (Run DM)

This run was designed to compare the parameterization methods with observations. The observational period was 12 days and was characterized by strong diurnal and synoptic scale forcing. The initial observed mixed layer was 20 meters deep with a temperature of 7.7 C, which were the initial conditions used in PROG. For CONS

and DIAG the top 50 meters of the initial observed temperature profile was averaged which gave $T_1(0)$ = 7.2 C and h(0) = 50 m (see Table III).

The back flux was held constant in this run also. Since the magnitude of the back flux depends on the SST it seems preferable to compute it. However, several other properties also affect the back flux, such as surface air temperature and surface wind speed. To show this, typical five-day means and fluctuations for the means of the properties influencing the back flux were estimated from data collycted at Ocean Station NOVEMBER and described by Dorman (1974). Table IV shows the typical fluctuations of each property and the resultant variations of the back flux (ΔB), as computed from empirical formulas (see Wyrtki, 1965; Dorman, 1974). Note that changes in the back flux due to some variables are the same order of magnitude as the change due to SST and may therefore be important in controlling the back flux at NOVEMBER. However some of these variables were not available from the observations at Ocean Station PAPA. Thus the back flux could not be reliably determined and was instead held constant at Denman and Miyake's (1973) value of 80 ly day^{-1}.

CONS (figure 30) and DIAG (figure 31) mixed water warmed by insolation throughout the top OGCM layer so that the mixed layer temperature responded slowly to changes in insolation and surface wind speed. In addition, $F_{1\frac{1}{2}}$ was usually positive using CONS and h was usually less than Δz_1 using DIAG, so that the diffusive parameterization for the flux (14) was used. On the other hand, shallowing of the mixed layer in PROG (figure 32) restricted mixing of insolation to a pro-

gressively thinner layer so that the mixed layer became warmer than T_1. The mixed layer depths in PROG and DIAG were in good agreement when h was small during the day, and reflected the tendency for the mixed layer depth of PROG to approach the diagnostic mixed layer depth during shallowing as was observed in runs T3 and D2. During periods of deepening, the mixed layer depth of PROG was limited by entrainment of cold quiescent water, while DIAG ignored any pre-existing thermal structure and the mixed layer grew to large depths.

All parameterization methods showed a warming trend relative to the observations, which may have been due to several factors. A cyclonic surface wind field associated with synoptic disturbances causes a divergence of ocean surface water and consequent upwelling. The ascent of cold water and its entrainment into the mixed layer results in cooler mixed layer temperatures than predicted by a one dimensional model. If this was the case the value of 80 ly day^{-1} for the back flux used by Denman and Miyake (1973) may have been accurate. If, on the other hand, large scale dynamics were not responsible for the difference, then B may have been too small. PROG and KIM were therefore rerun using B = 160 ly day^{-1}. The results showed greater agreement in T_m, while h changed little because the amount of entrainment due to convection was small.

V. DISCUSSIONS AND CONCLUSIONS

In most of the experimental runs the forcing was such that downward heat flux due to entrainment did not occur between the top two OGCM layers. The exception was the run with only wind forcing (run T2), in which downward heat flux did occur when using the predetermined mixed layer depth (CONS) and prognostic mixed layer depth (PROG) parameterization methods.

The results of the transient runs do not suggest a superior parameterization method. The sea surface (SST) results obtained using CONS and the diagnostic mixed layer depth parameterization method (DIAG) were the same as the results obtained using the OGCM with only diffusive mixing (DIFF) when insolation was present (runs T1 and T3). On the other hand PROG responded to both wind and convective mixing but underwent repeated, spurious convective adjustment in run T1.

It is also unclear which parameterization method should be considered superior from the results of the diurnally forced runs (D1 and D2). Using PROG, the mixed layer was able to shallow appreciably when wind effects were excluded (run D1) so that the SST warmed significantly more than it did using the other two parameterization methods and resembled the SST results obtained using the mixed layer only model (KIM). Using PROG and including wind forcing (run D2) shallowing was reduced during the day, and diurnal warming of the SST was not very different from the results obtained using the other parameterization

methods. However, a spurious longer time scale warming did occur which was not observed when the other methods were used.

The run using Denman and Miyake's (1973) observations (DM) provides the clearest indication of a superior parameterization method: the prognostic mixed layer depth method. The shallow mixed layer depth using PROG allows much more variability of the SST in response to forcing. In contrast, the SST response using CONS and DIAG is small due to the large depth over which mixing occurs (the top OGCM layer) in these methods. Although a gradual warming trend of the SST was observed, the results using PROG resembled the observations much more closely than did the results obtained from CONS or DIAG.

Based on the experimental results, the prognostic mixed layer parameterization method is superior to either the predetermined or the diagnostic mixed layer depth parameterization methods. The inferior performance of CONS and DIAG is due to their inability to parameterize wind and convective mixing in some important conditions such as strong insolation, weak wind or weak back flux. If, when using PROG, the mixed layer depth is less than the uppermost OGCM layer depth, insolation and back flux cause changes in the temperature uniformly over the mixed layer, while these changes are distributed over the whole uppermost OGCM layer when either CONS or DIAG is used. In other words, if arbitrarily many OGCM layers were chosen to represent the upper layers of the ocean, all three methods might give similar results because the mixed layer would always be close in depth to an integer number of OGCM layers. However, an OGCM which is to be economical for runs of many time steps must have only a few

layers, with correspondingly coarse vertical resolution of the upper ocean.

Improvements to the predetermined and the diagnostic mixed layer depth parameterization methods are possible. One possibility is to reduce the uppermost OGCM layer depth and correspondingly increase the depth of the second OGCM layer. With the mixed layer and uppermost OGCM layer of similar size, better response of CONS and DIAG is to be expected. However, the effect on these parameterizations of a mixed layer which is significantly deeper than the top OGCM layer is uncertain. Another possible improvement is to use a more sophisticated parameterization for SST. One simple method is to linearly extrapolate SST at the sea surface through the arithmetic average of the top two OGCM layer temperatures at the base of the top layer ($T_{1\frac{1}{2}}$, $-\Delta z_1$) and the top layer temperature at the middle of the top layer (T_1, $-\frac{1}{2}\Delta z_1$). For given $T_{1\frac{1}{2}}$, the SST would then change twice as much as T_1. However under conditions where CONS or DIAG revert to DIFF, the SST will still only be responding to diffusive mixing. In DIAG further improvement to the SST can be made by linear extrapolation or interpolation of (T_1, $-\Delta z_1$) and (T_1, $-\frac{1}{2}\Delta z_1$) to the mixed layer base. Since the mixed layer depth is the result of wind and convective mixing, the SST will reflect changes in these processes to a certain extent. But if insolation exists, diffusive mixing may again replace convective and wind mixing, in which case the mixed layer depth will not be available and some other method of finding the SST must be used. It is clear then that only the prognostic method of determining the mixed layer depth results in an SST which is continuously responsive

to wind and convective mixing when winds are light, back flux is small or insolation is large.

Although the prognostic mixed layer depth parameterization appears to be the most satisfactory method when used in a coarse vertical resolution OGCM for runs of several days, certain behavior such as the repeated convective adjustment in run T1 and the slow warming in run D2 suggest the possibility of undesirable longer time scale behavior when the model is run for longer periods. PROG should be carefully tested in runs of one or more years and compared to observations in order to examine its response to the combined influence of diurnal, synoptic and seasonal scale forcing before being used to predict SST independently of observations.

Table I. Summary of methods used to calculate the sea surface temperature (SST) and mixed layer depth (h) by three mixed layer parameterization methods (CONS, DIAG and PROG), by a diffusive parameterization (DIFF), and by a mixed layer model (KIM).

	SST	h
CONS	Equivalent to top OGCM layer temperature (T_1)	Predetermined as depth of base of one or more layers of oceanic general circulation model
DIAG	Equivalent to T_1	Diagnostically determined (Monin-Obukhov length)
PROG	Prognostically determined	Prognostically determined
DIFF	Equivalent to T_1	Not determined
KIM	Prognostically determined	Prognostically determined

Table II. The experimental runs including types of forcing. The three parameterization methods are CONS, DIAG and PROG. DIFF is the oceanic general circulation model (OGCM) with diffusive mixing and KIM is the mixed layer model.

Experimental Runs

	T1	T2	T3	D1	D2	DM
CONS	A,D	E	A,D,E	B,D	B,D,E	B,C,D,F
DIAG	A,D	E	A,D,E	B,D	B,D,E	B,C,D,F
PROG	A,D	E	A,D,E	B,D	B,D,E	B,C,D,F
DIFF	A,D	-	---	B,D	B,D,E	B,C,D
KIM	A,D	E	A,D,E	B,D,	B,D,E	B,C,D,F

Code: A - Constant insolation (R_0)

B - Diurnally varying R_0

C - Synoptically varying R_0

D - Constant back flux (B)

E - Constant surface wind speed (U_s)

F - Variable U_s

Table III. Initial and Boundary Conditions for the Experimental Runs

	Boundary Conditions			Initial Conditions							
					OGCM Layer Temperatures						
	Daily average insolation $(\bar{R}_0)$ (ly day^{-1})	Back flux (B) (ly day^{-1})	Surface wind speed (U_s) (m s^{-1})	Mixed layer temperature (T_m) (°C)	T_1 (°C)	T_2 (°C)	T_3 (°C)	T_4 (°C)	Mixed layer depth (h) (m)	Run duration (hr)	Timestep (Δt) (hr)
Transient Runs											
T1	300	300	0.0	7.0	7.0	6.0	5.0	4.0	50	120	1
T2	0	0	7.5	7.0	7.0	6.0	5.0	4.0	50	120	1
T3	300	300	0.0	7.0	7.0	6.0	5.0	4.0	50	120	1
Dirunal Runs											
D1	300	300	0.0	7.0	7.0	6.0	5.0	4.0	50	120	1
D2	300	300	7.5	7.0	7.0	6.0	5.0	4.0	50	120	1
Denman-Miyake											
DM	---	80	---	7.7	7.2	4.5	4.0	4.0	20	287	1

Notes:
1. For symbol definitions refer to List of Symbols
2. Transient runs: $R_0 = \bar{R}_0$
3. Diurnal runs: $R_0 = -\bar{R}_0 \pi \cos(2\pi t/t^*)$ - day ($t = 0$ at midnight)
   $= 0$ - night
4. Parameter values: $\beta = 0.2\ m^{-1}$, $\gamma = 0.05\ m^{-1}$, $p = 0.15$, $n = 3.0$, $\kappa = 0.0001\ m^2 s^{-1}$

Table IV. Typical fluctuations of the heat flux across the ocean surface (back flux) on a synoptic time scale at Ocean Station November in May. The change in the back flux B due to a change in one of the variables affecting it (ϕ) is $\Delta B = (\partial B/\partial \phi)\Delta\phi$. Expressions for $\partial B/\partial \phi$ are derived from the empirical formulas for B of Wyrtki (1965) and Dorman (1974).

Variable (ϕ)	Typical value of ϕ ($\bar{\phi}$)	Typical fluctuation of ϕ ($\Delta\phi$)	Magnitude of a typical fluctuation of B due to $\Delta\phi$ ($\lvert\Delta B\rvert$) (ly day^{-1})
Surface wind speed (m s^{-1})	5	5	217.3
Sea surface temperature (°C)	19	2	145.3
Surface air temperature (°C)	18	6	185.6
Surface specific humidity (g kg^{-1})	9.3	3	163.9
Surface atmospheric pressure (mb)	1000	20	13.9
Percent low cloud cover	.5	.4	86.6

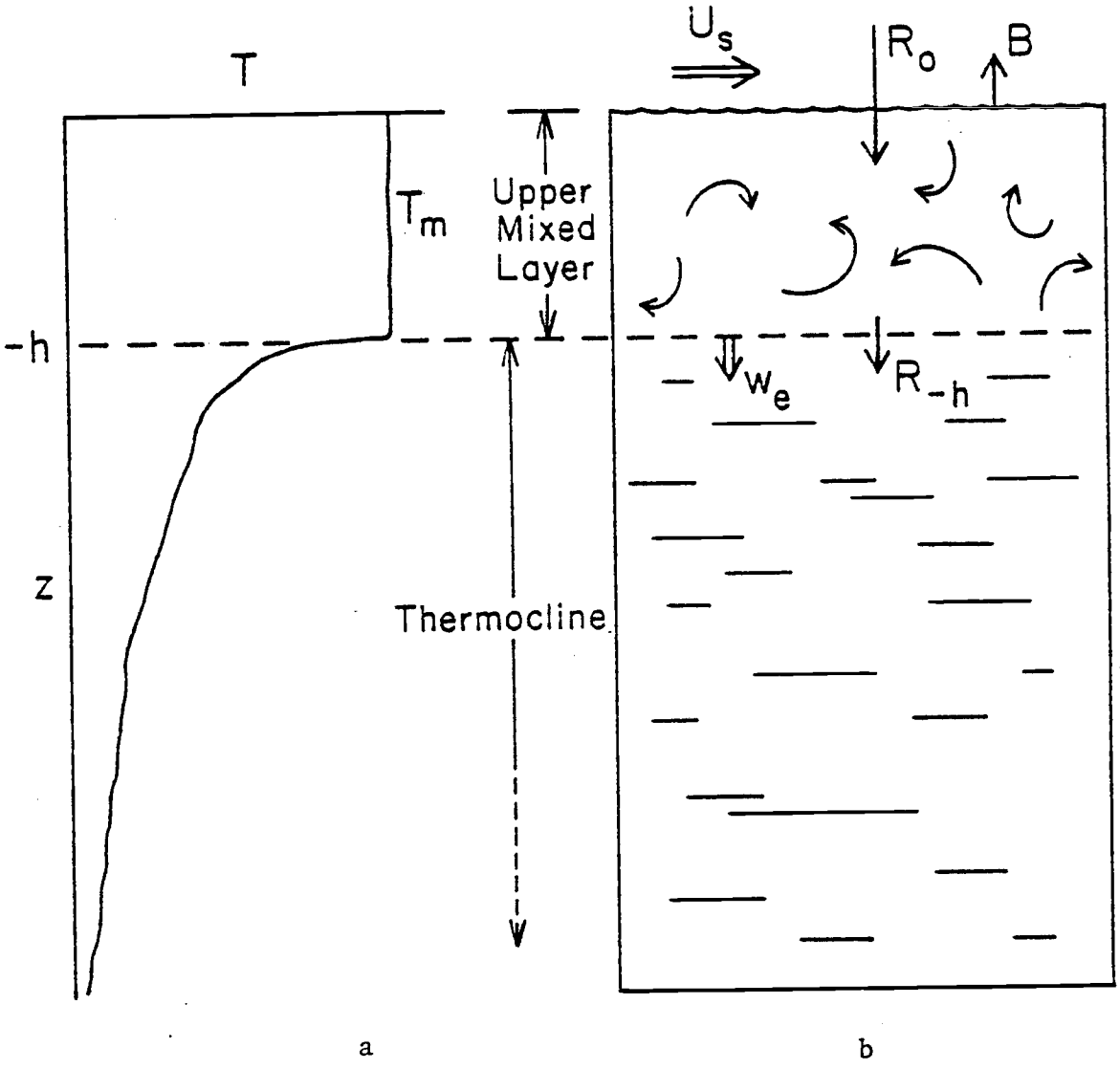

Fig. 1. a. Vertical temperature profile of a typical upper oceanic mixed layer of temperature T_m and depth h. b. Typical mixed layer showing turbulent motions with quiescent stratified water below, the insolation at the sea surface and mixed layer bottom, R_0 and R_{-h} respectively, the back flux B, surface wind U_s, and the entrainment rate w_e.

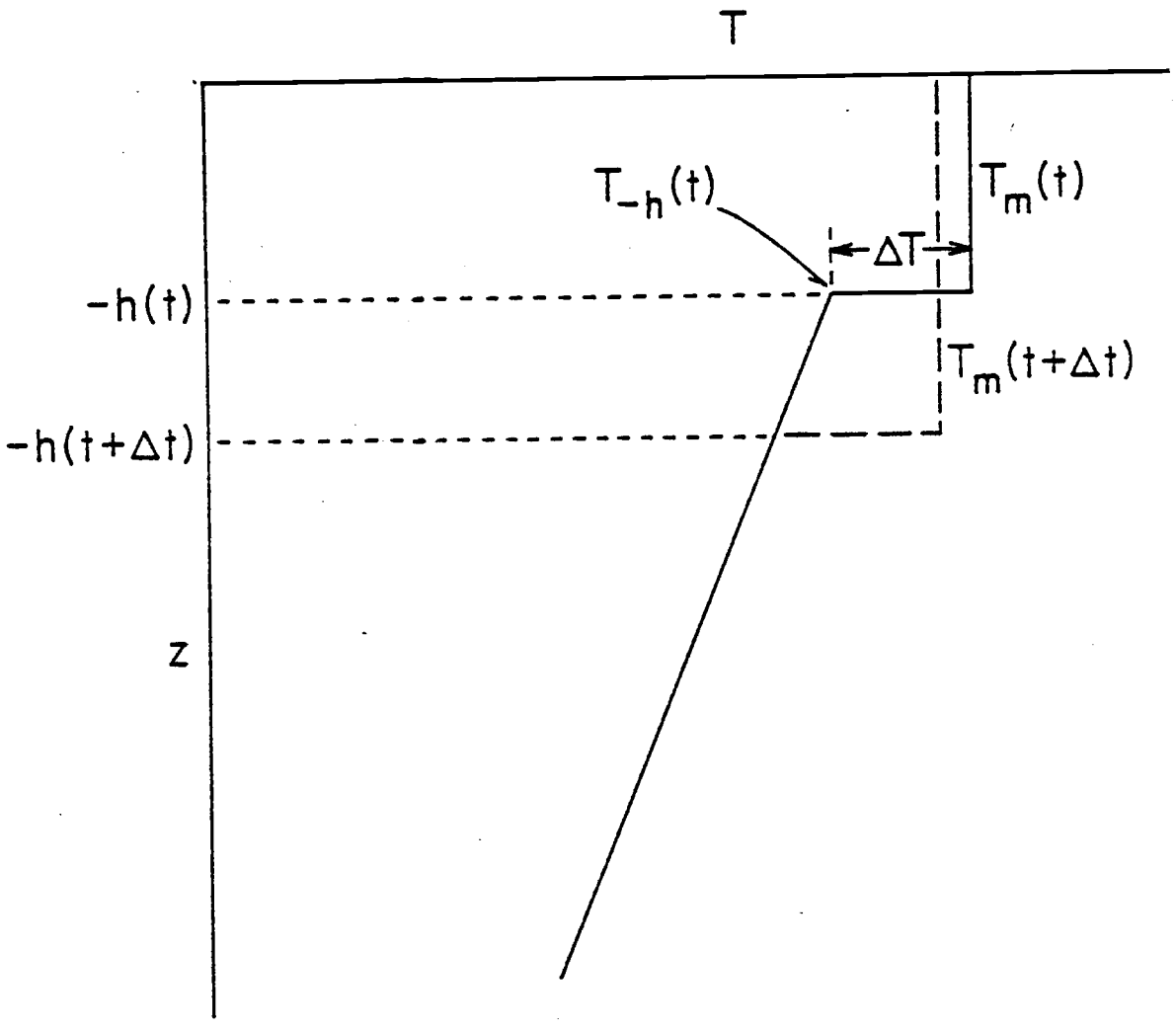

Fig. 2. Temperature profile of a one dimensional mixed layer model at time t (solid line) and after one time step at time $t + \Delta t$ (dashed line). The temperature jump scross the interface separating turbulent and quiescent water is ΔT where T_{-h} is the temperature of the quiescent water and T_m is the mixed layer temperature.

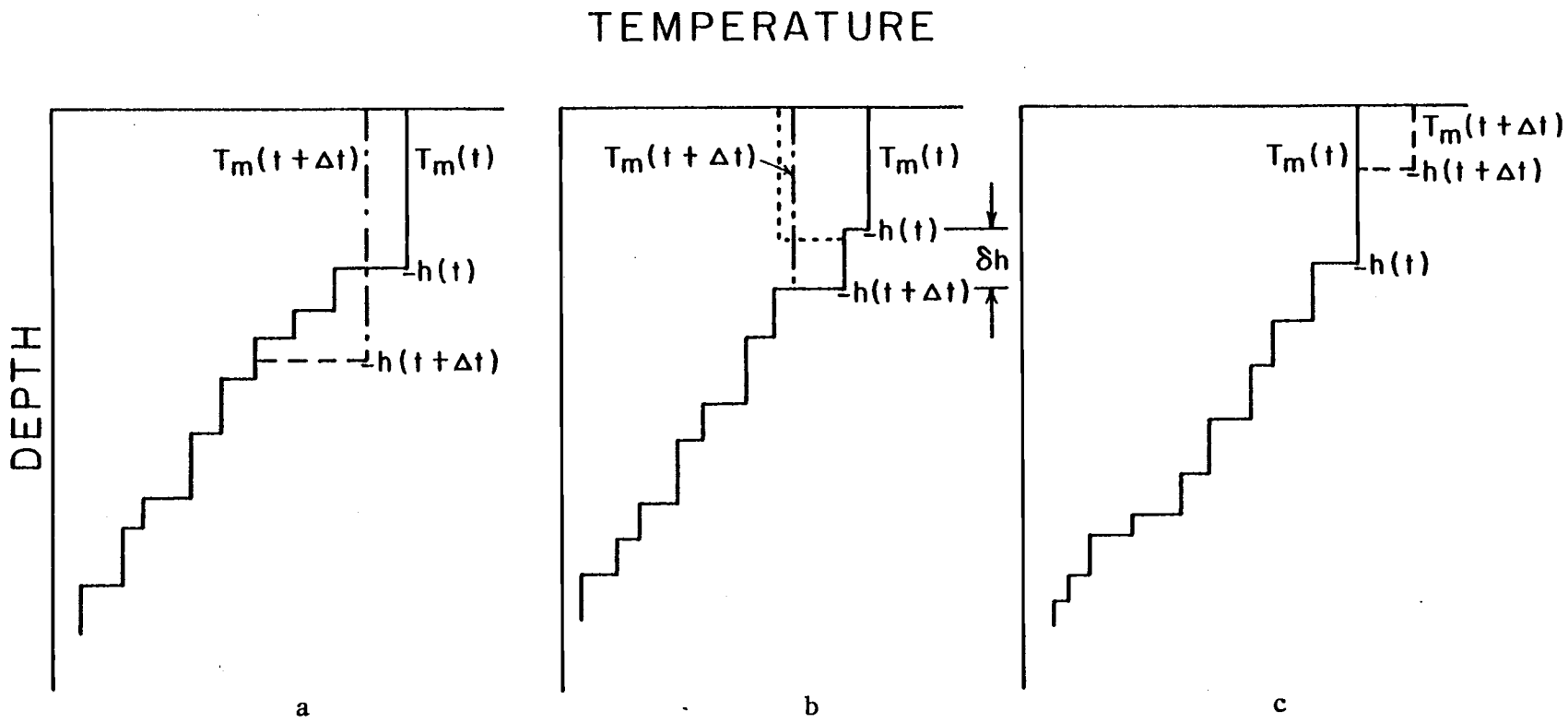

Fig. 3. Temperature profiles of the mixed layer model of Kim (1976) showing a. entrainment, b. shallowing and cooling (dotted line) followed by convective adjustment (dotted and dashed line) and c. shallowing and warming. The mixed layer temperature and depth are T_m and h, respectively.

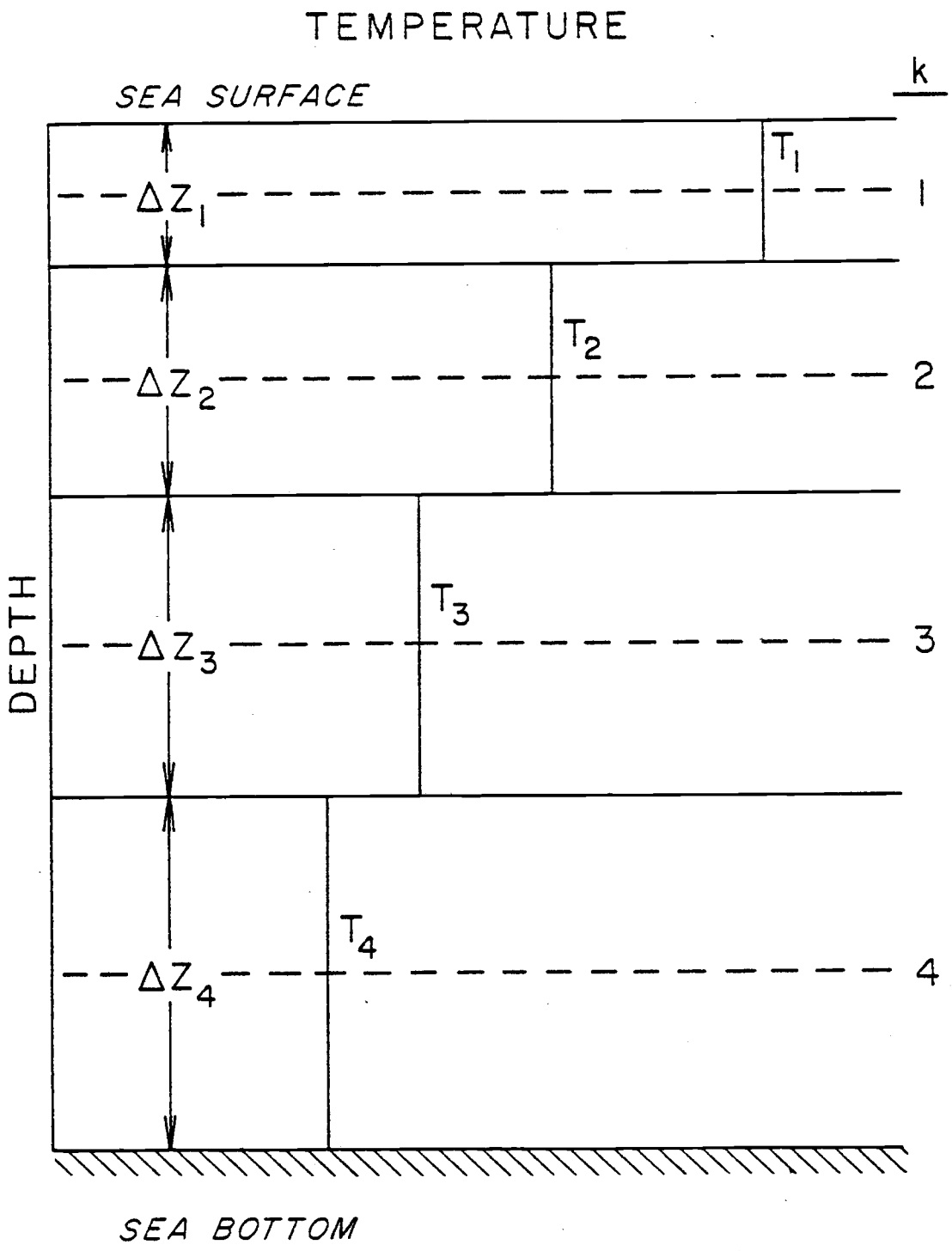

Fig. 4. Representation of the layer temperatures T_k and corresponding layer thicknesses Δz_k of the four layer OGCM of Kim and Gates (1978) where k may have the integer values 1, 2, 3, 4 corresponding to the four layers.

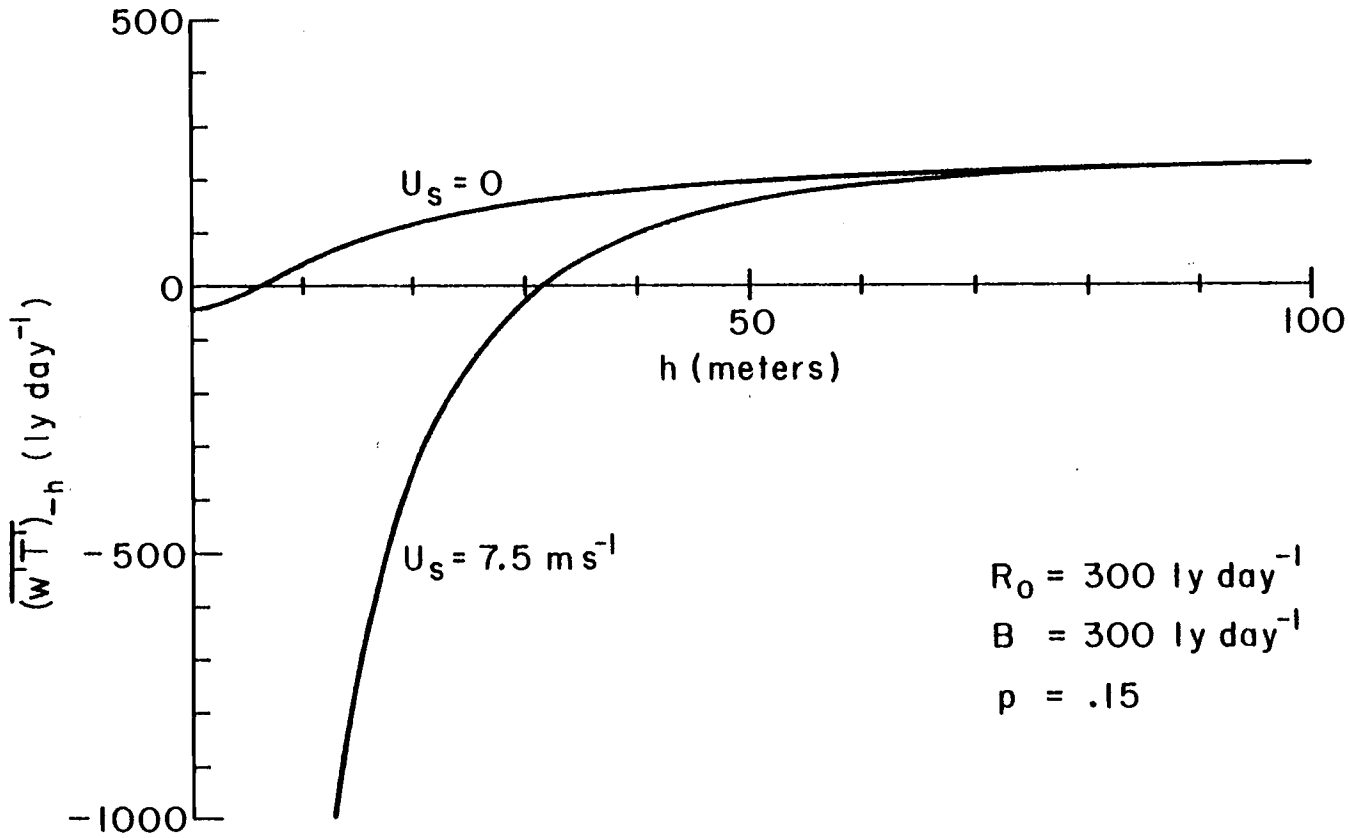

Fig. 5. The entrainment flux $(\overline{w'T'})_{-h}$ as a function of the mixed layer depth h for two values of the surface wind speed U_s, where R_0 and B are the surface insolation and back flux respectively and p is the penetration factor.

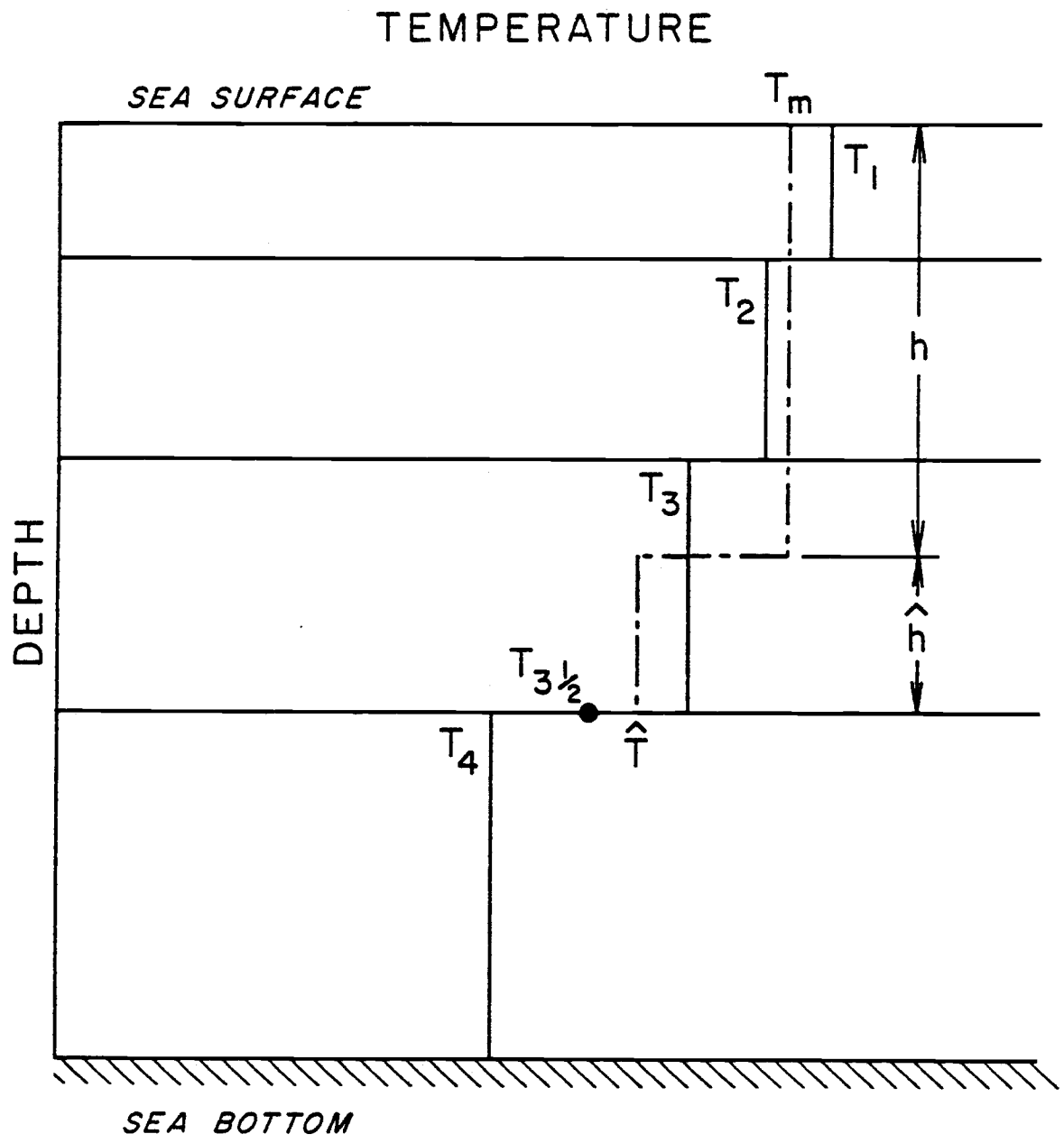

Fig. 6. The temperature profile of the embedded prognostic mixed layer depth parameterization method. The OGCM layer temperatures are given by T_k with k = 1,2,3,4, the mixed layer temperature by T_m and the depth by h. The arithmetic average of the temperature of the OGCM layer containing the mixed layer base and the temperature of the OGCM layer underneath (T_L and T_{L+1}) is $T_{L+\frac{1}{2}}$ where L = 3 in this figure (see text). The temperature $\hat{T}$ of the layer $\hat{h}$ is given by (19).

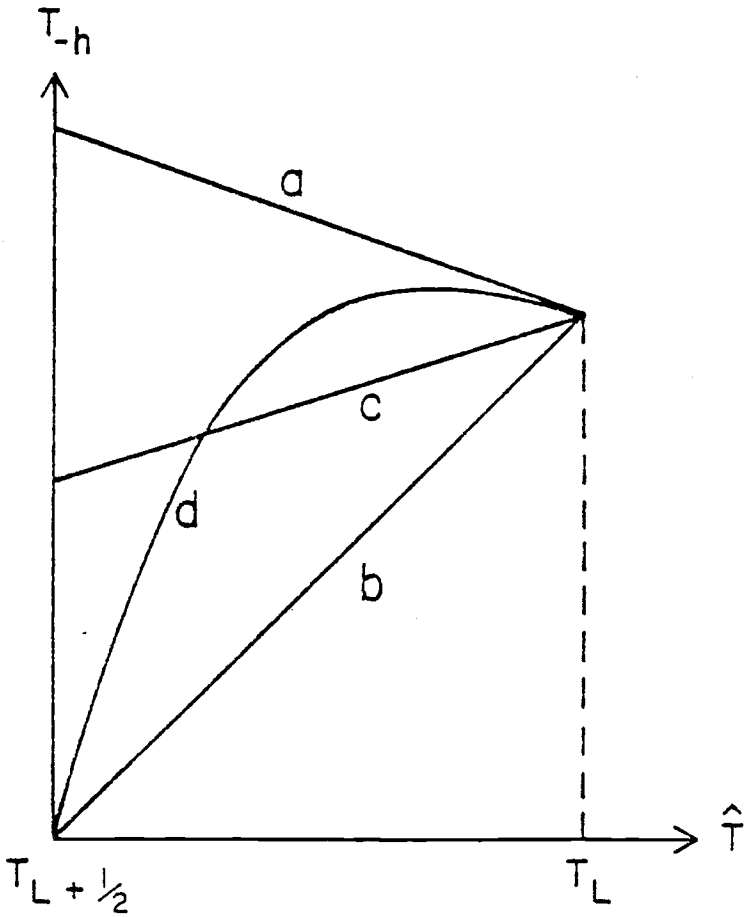

Fig. 7. The estimation of T_{-h} from the OGCM thermal structure:

a. $T_{-h} = T_m$

b. $T_{-h} = \hat{T}$

c. $T_{-h} = \frac{T_m + \hat{T}}{2}$

d. $T_{-h} = \frac{\hat{T} - T_{L+\frac{1}{2}}}{T_L - T_{L+\frac{1}{2}}} T_m + \frac{T_L - \hat{T}}{T_L - T_{L+\frac{1}{2}}} \hat{T}$

The various temperatures are defined in the text and in the list of variables.

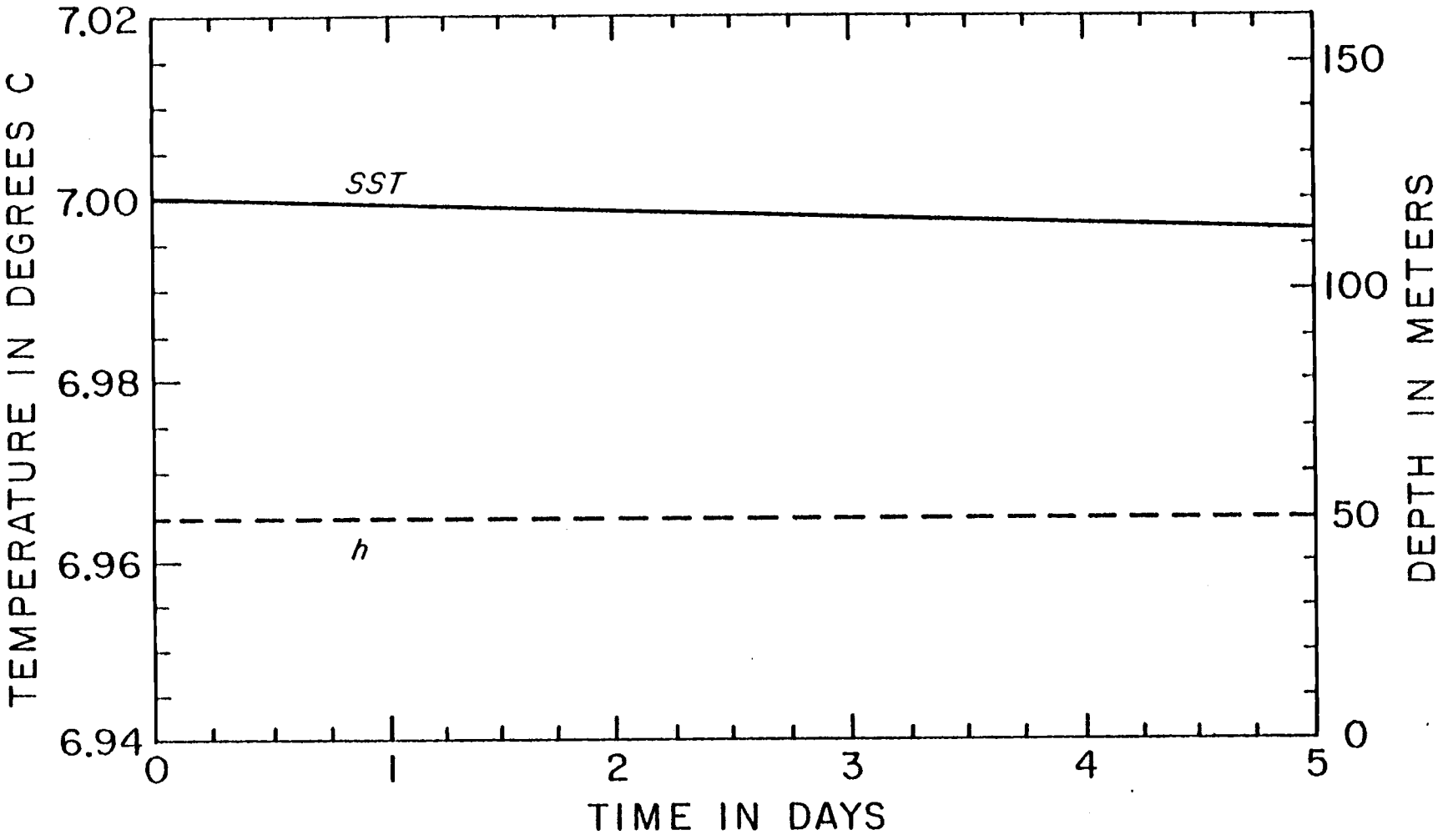

Fig. 8. Time series of sea surface temperature (SST) and mixed layer depth h from run T1 using diffusive mixing (DIFF) and from runs T1 and T3 using the predetermined mixed layer depth parameterization method (CONS).

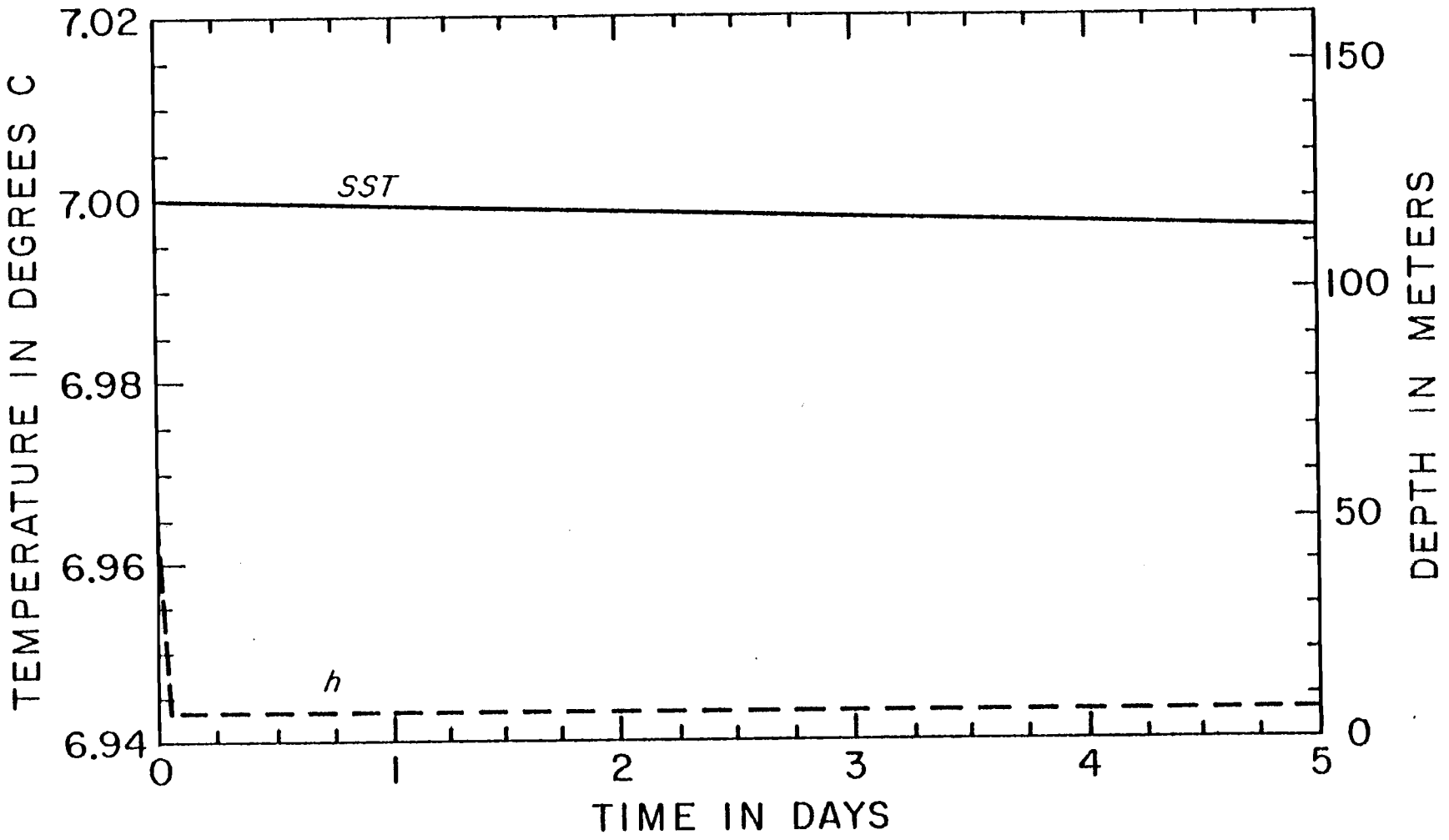

Fig. 9. Time series of SST and h from run T1 using the diagnostic mixed layer depth parameterization method (DIAG).

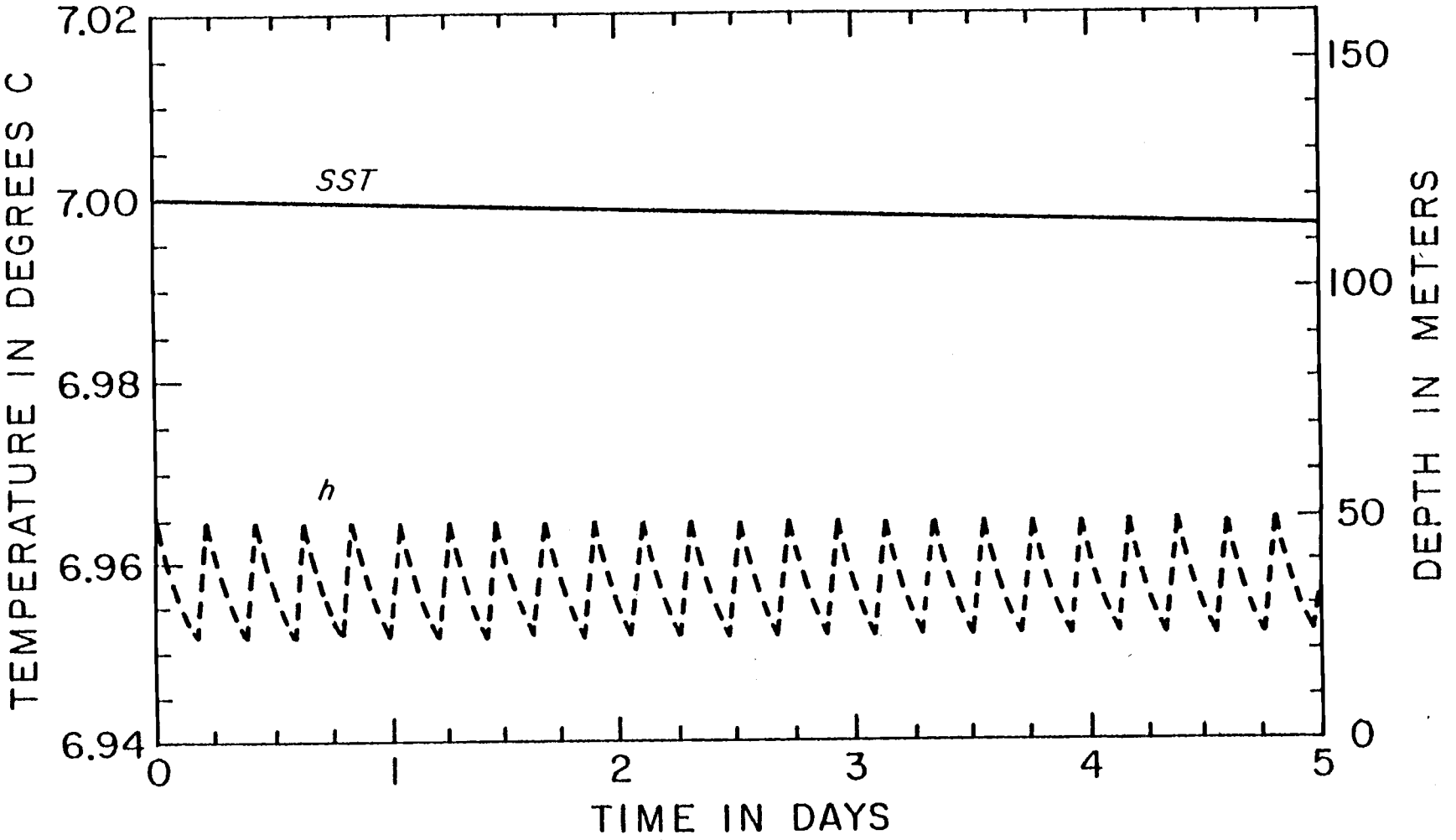

Fig. 10. Time series of SST and h from run T1 using the prognostic mixed layer depth parameterization method (PROG).

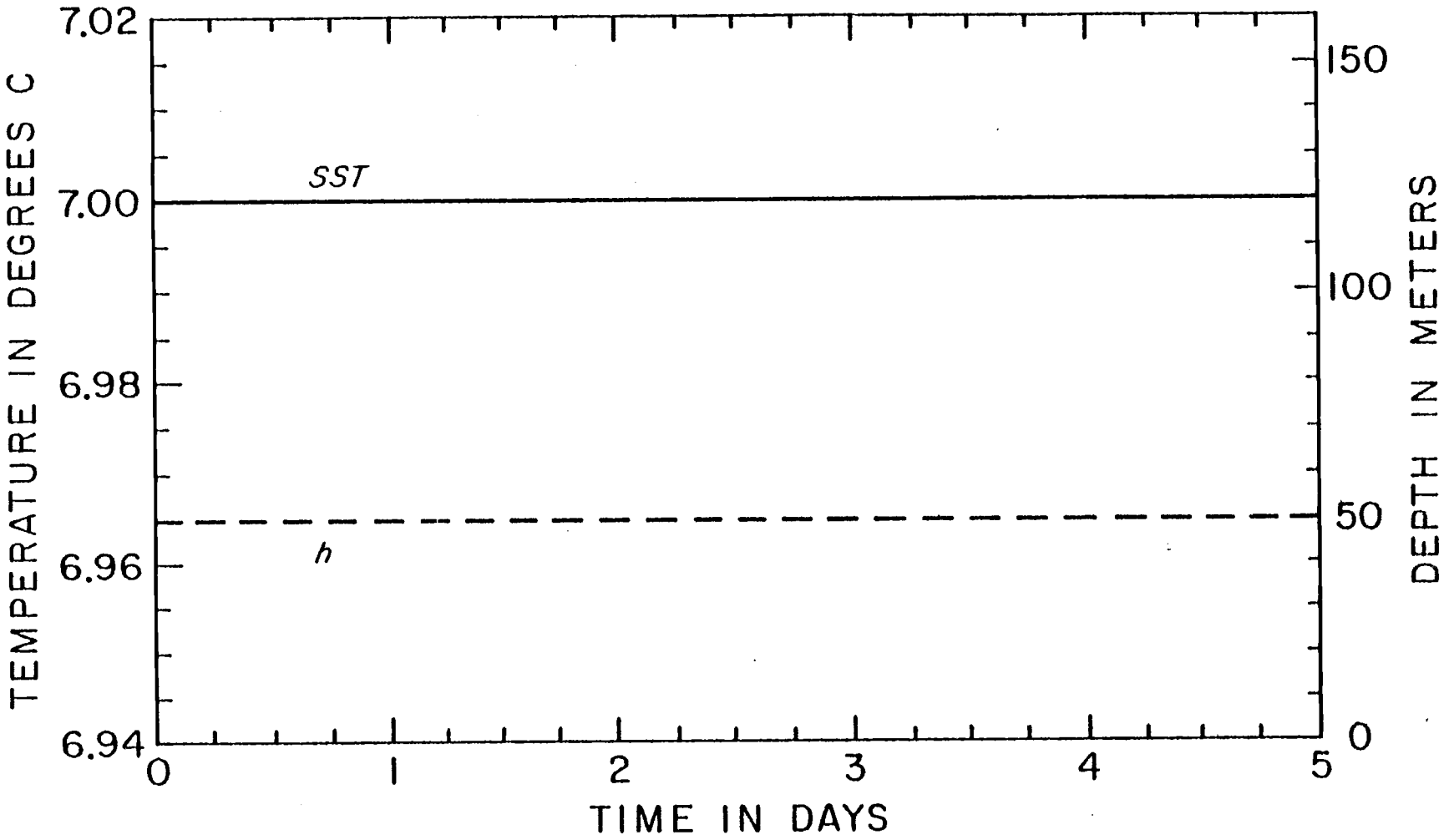

Fig. 11. Time series of SST and h from run T1 and run T3 using the mixed layer model (KIM).

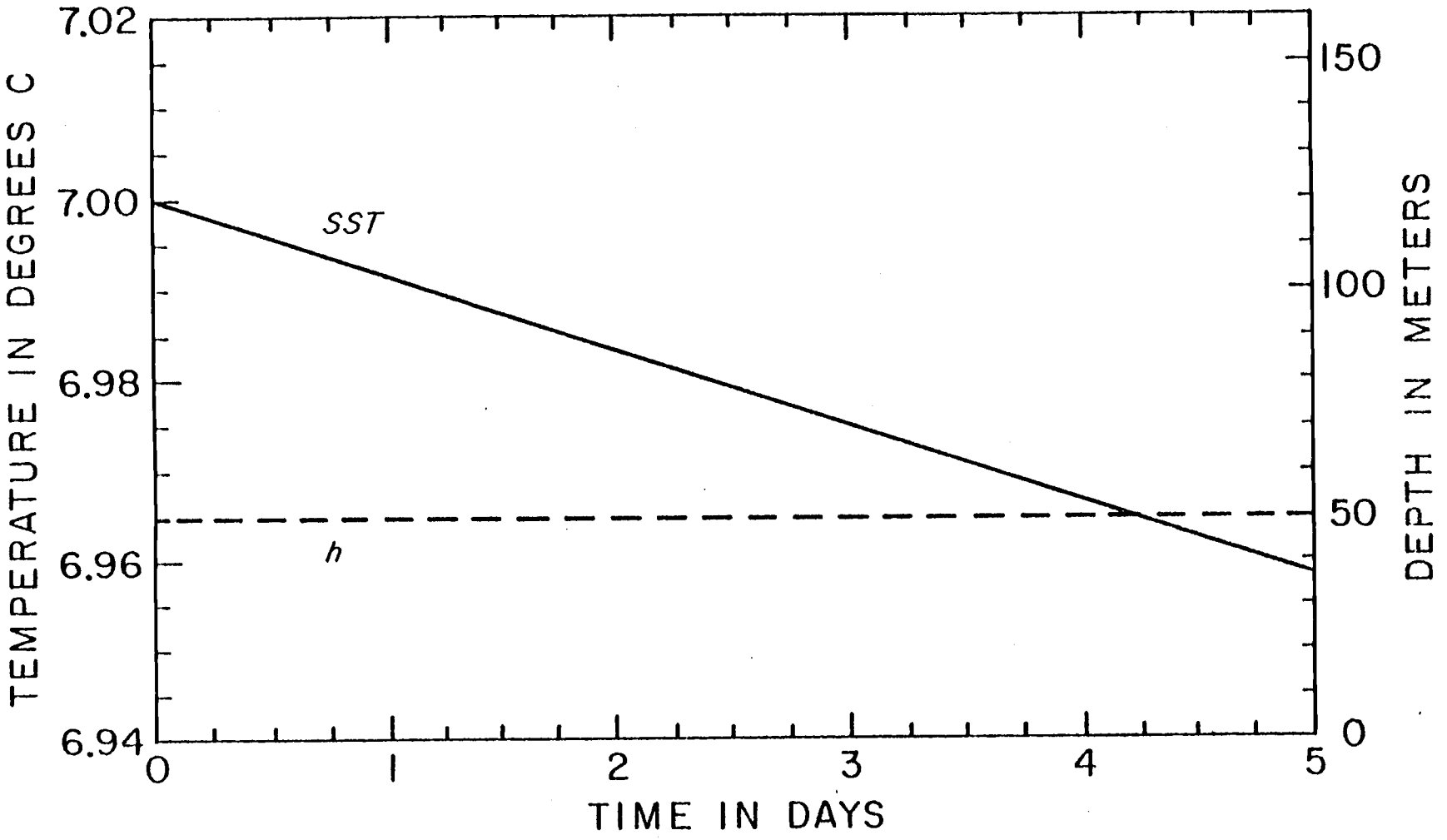

Fig. 12. Time series of SST and h from run T2 using CONS.

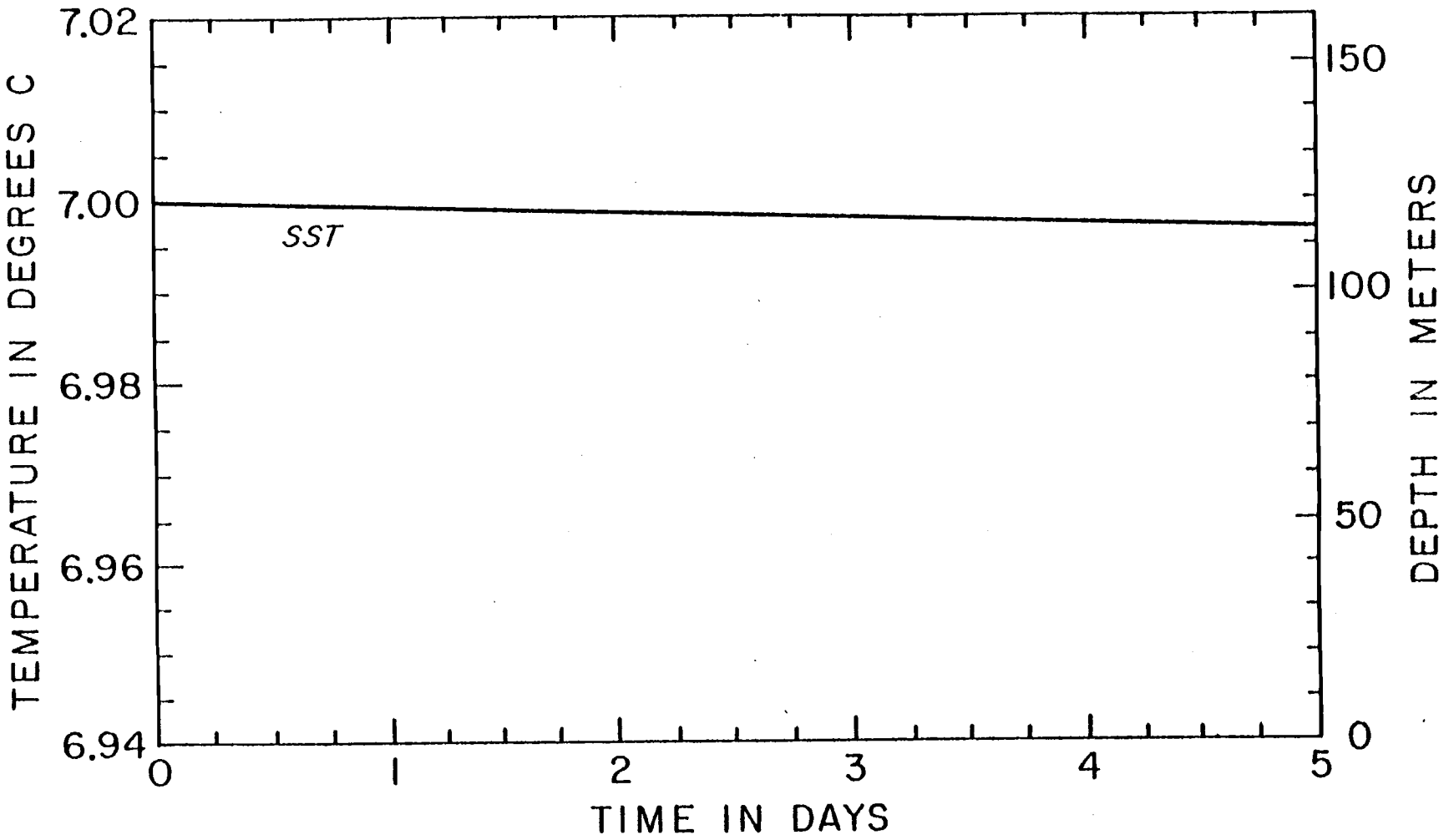

Fig. 13. Time series of SST from run T2 using DIAG. Note that since $R_0 = B = 0$, h is not computed.

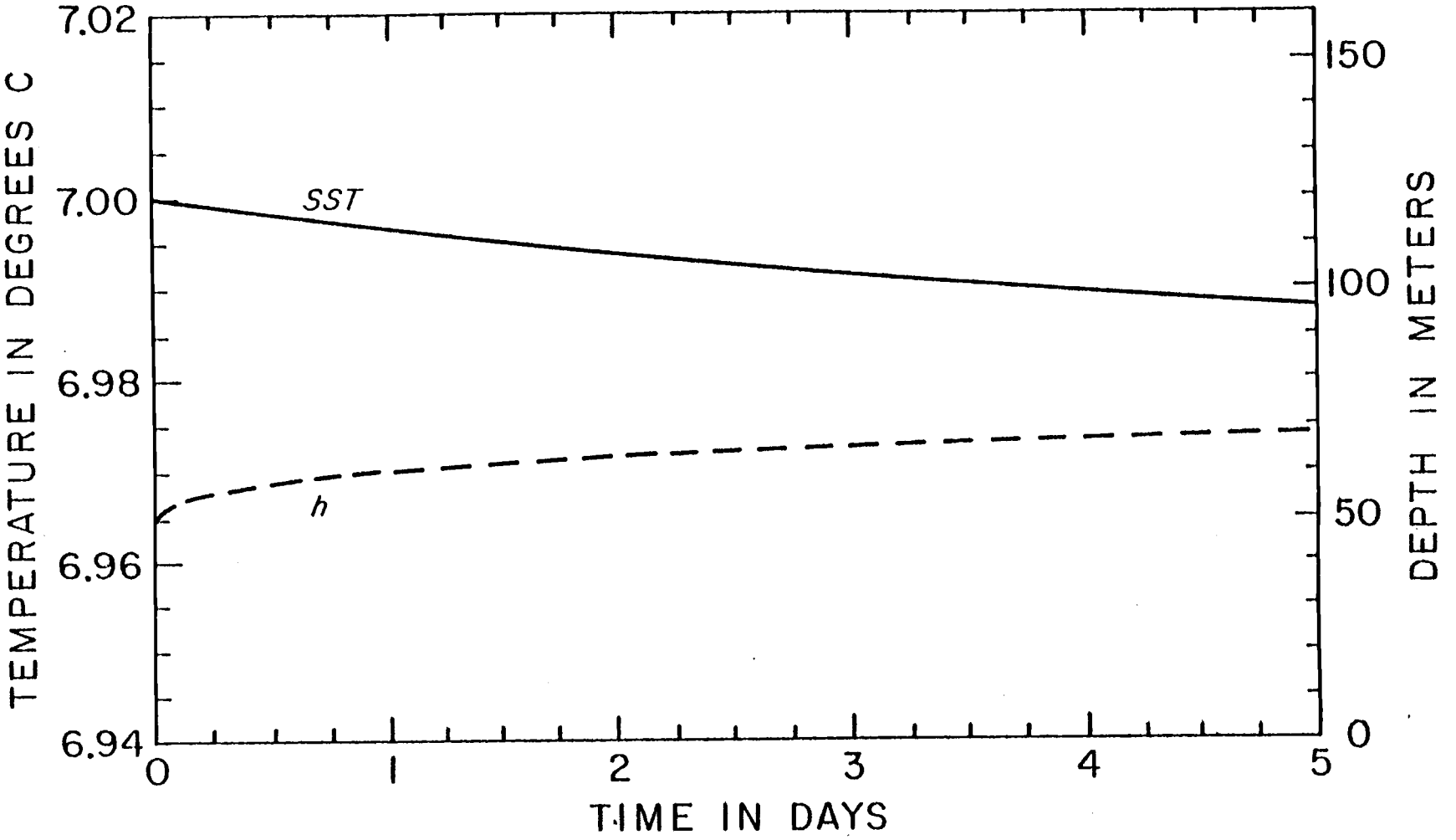

Fig. 14. Time series of SST and h from run T2 using PROG.

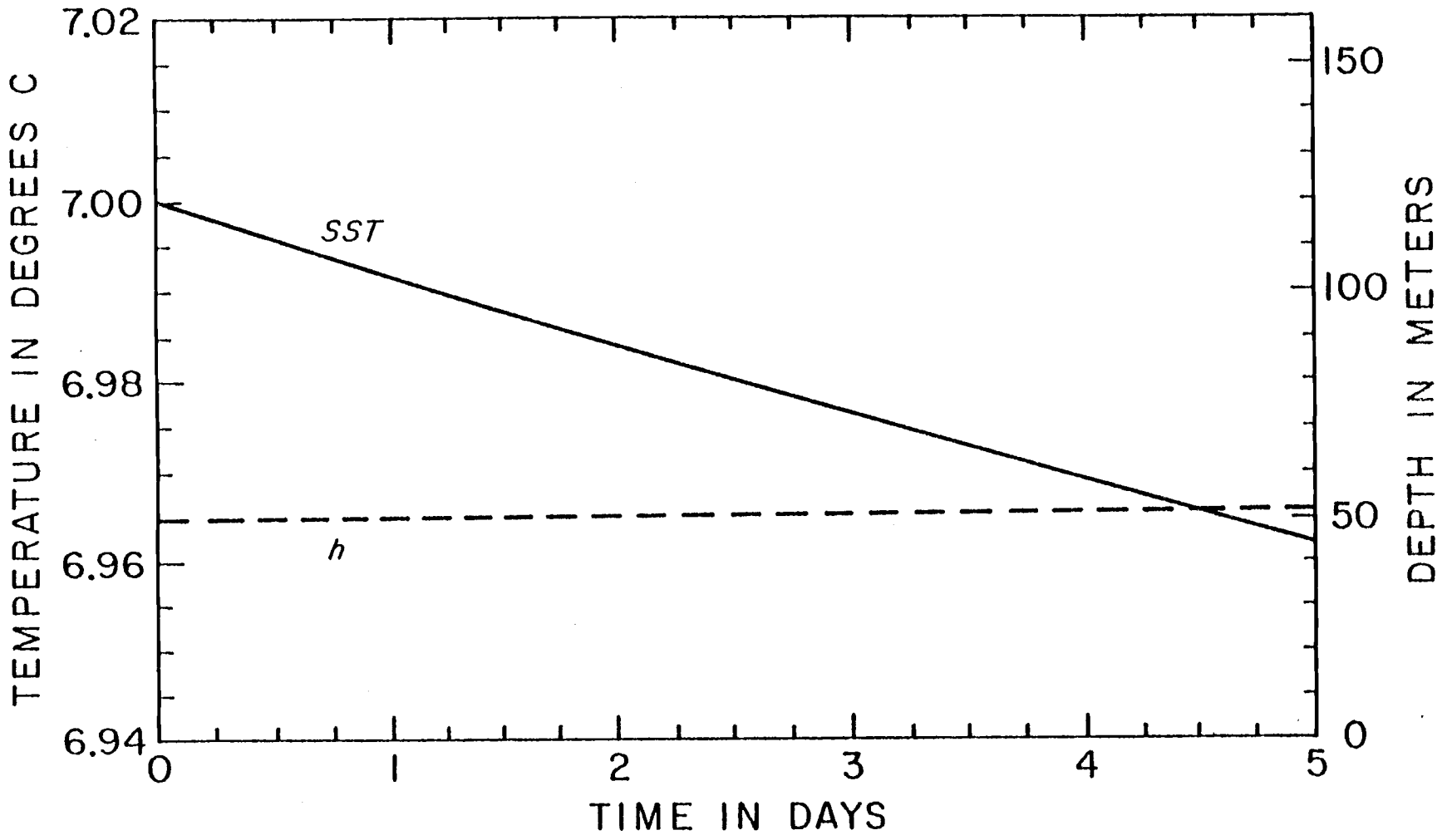

Fig. 15. Time series of SST and h from run T2 using KIM.

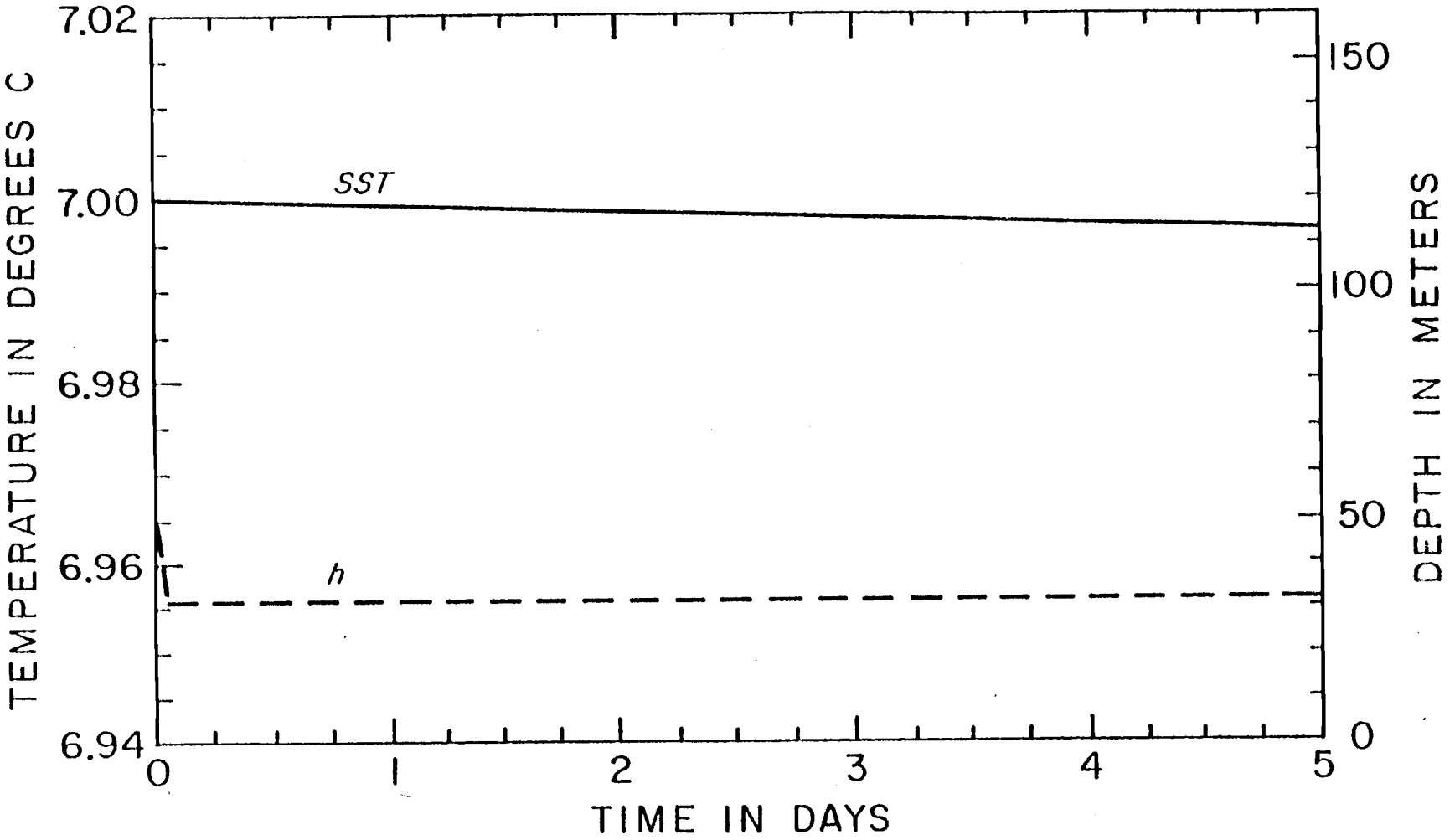

Fig. 16. Time series of SST and h from run T3 using DIAG.

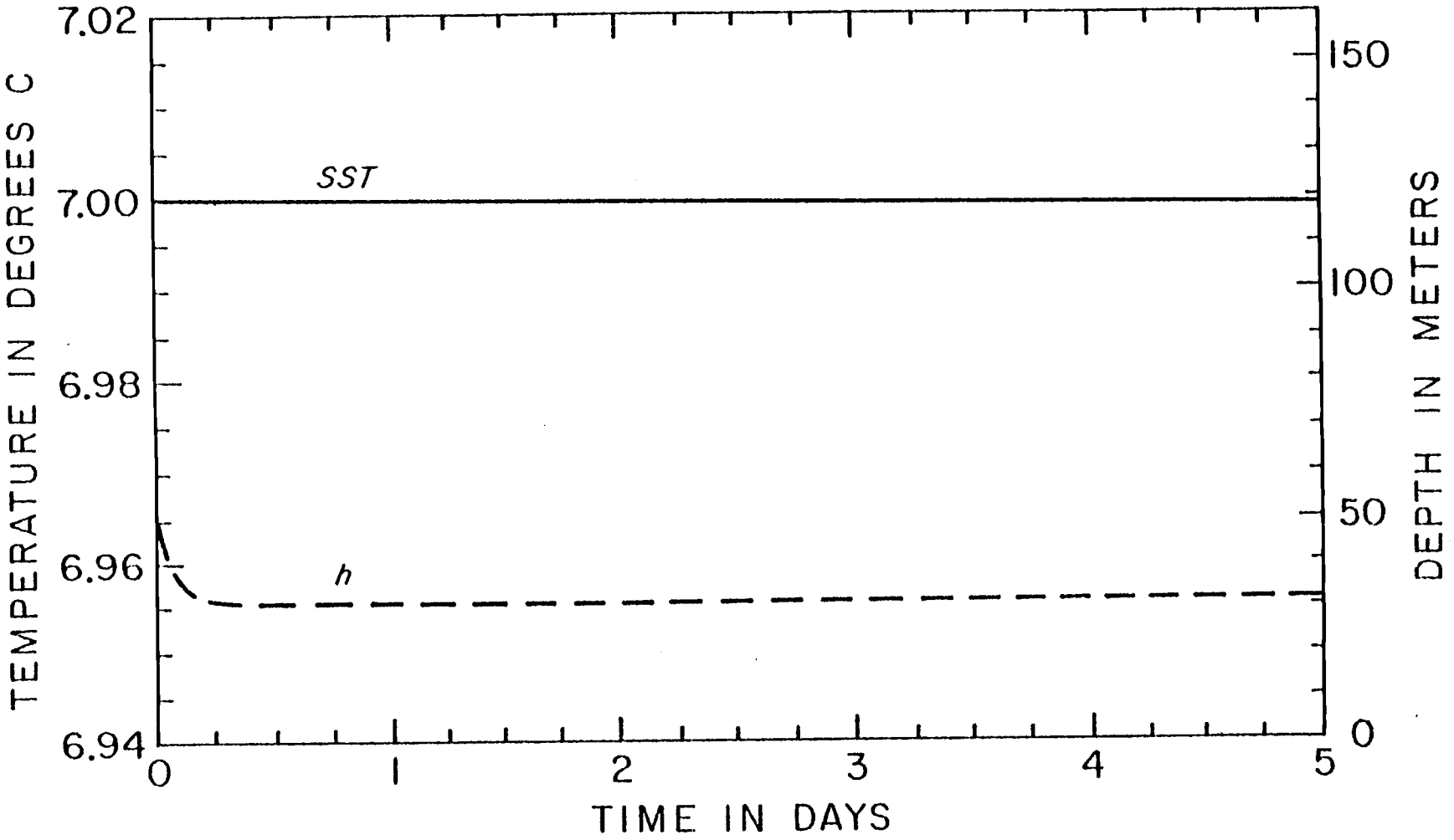

Fig. 17. Time series of SST and h from run T3 using PROG.

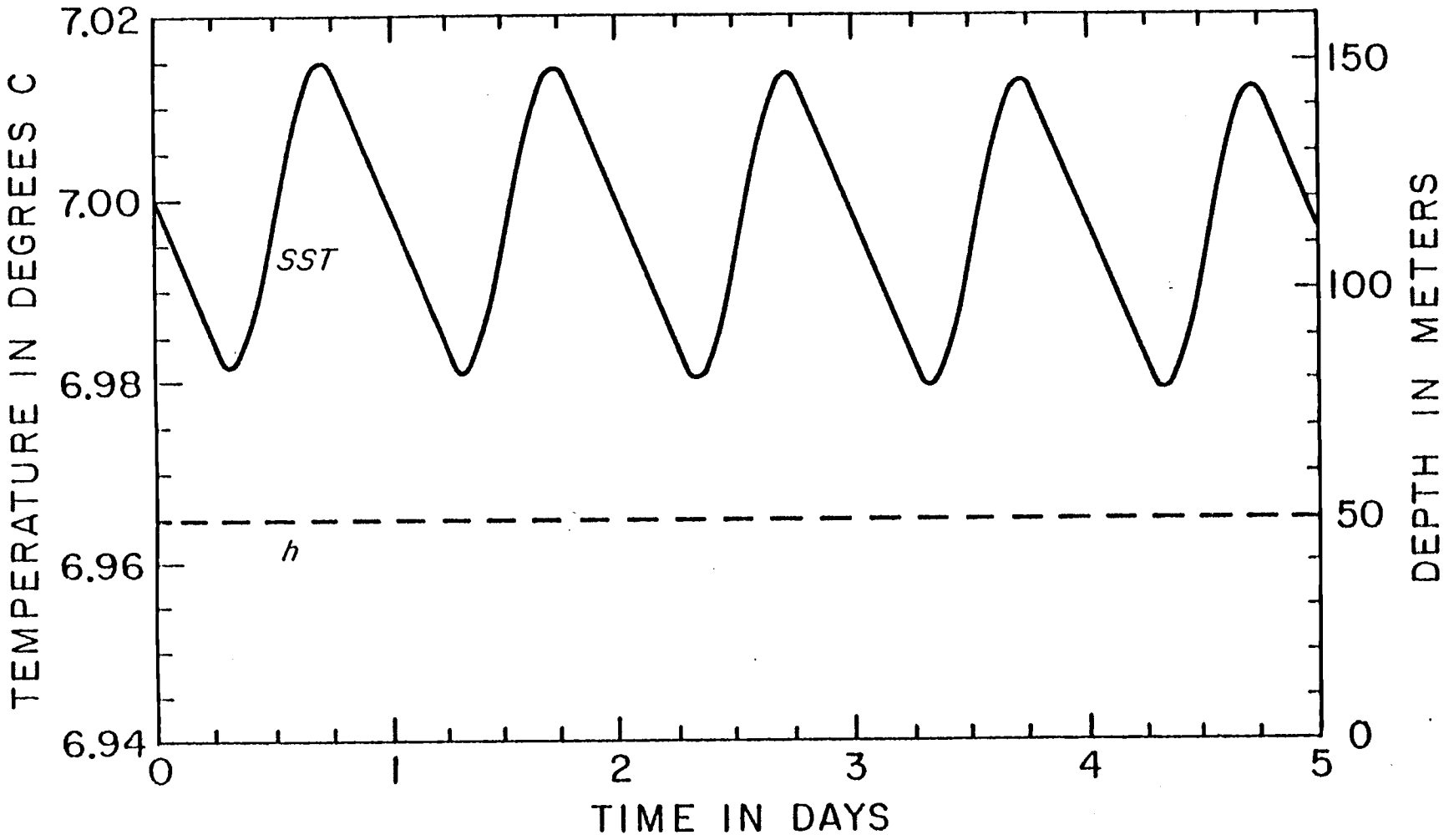

Fig. 18. Time series of SST and h from run D1 using DIFF.

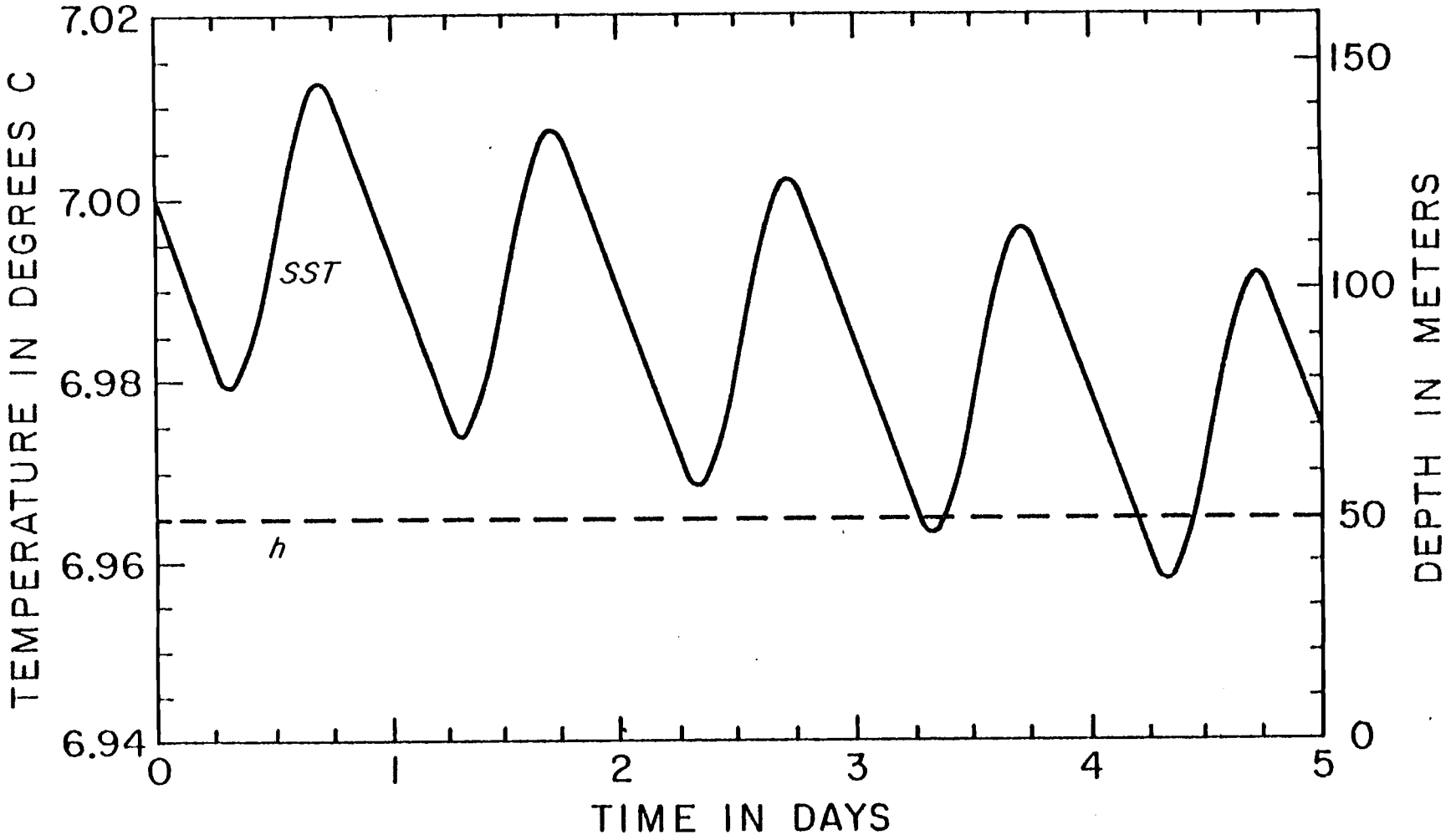

Fig. 19. Time series of SST and h from run D1 using CONS.

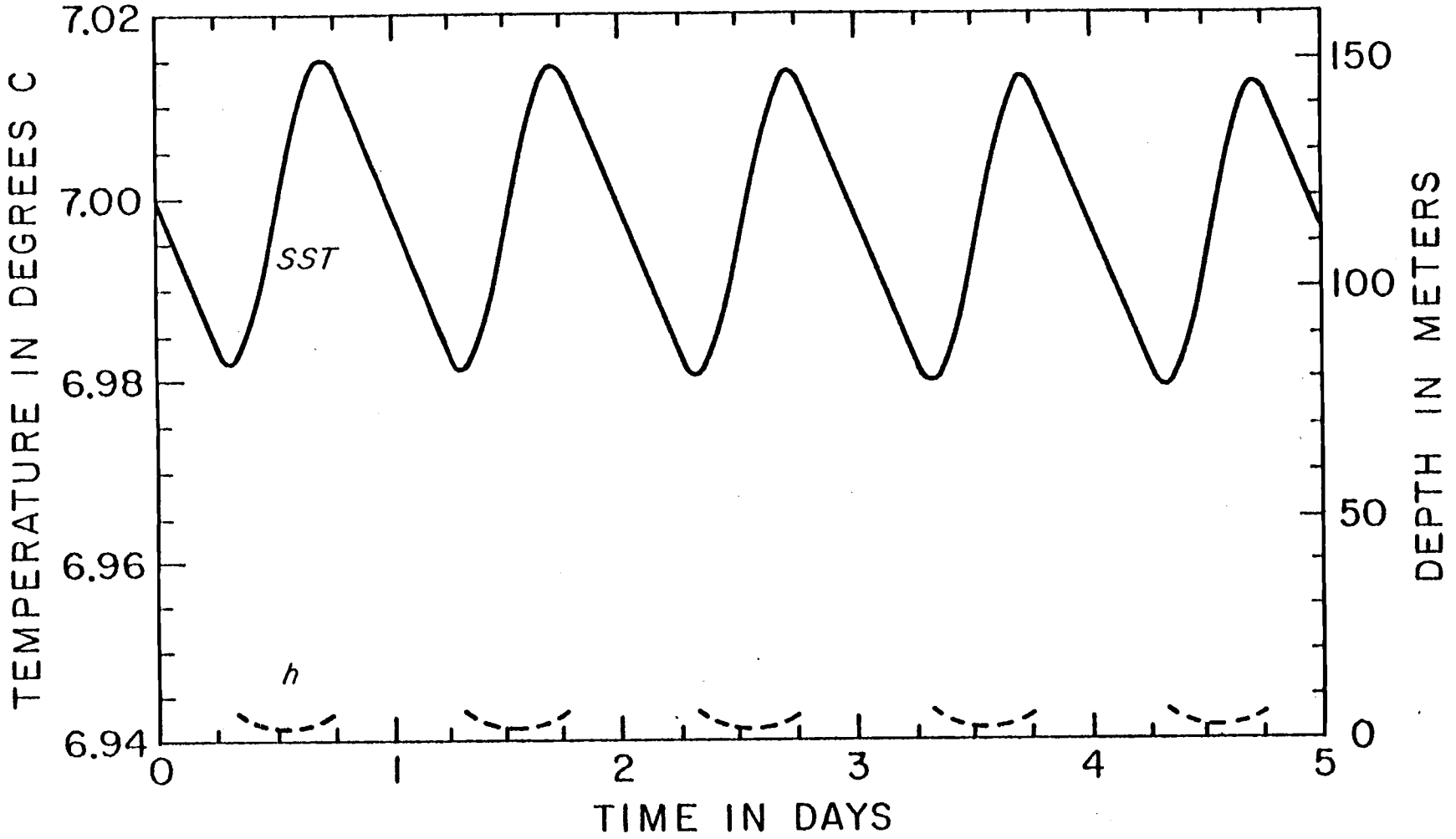

Fig. 20. Time series of SST and h from run D1 using CONS.

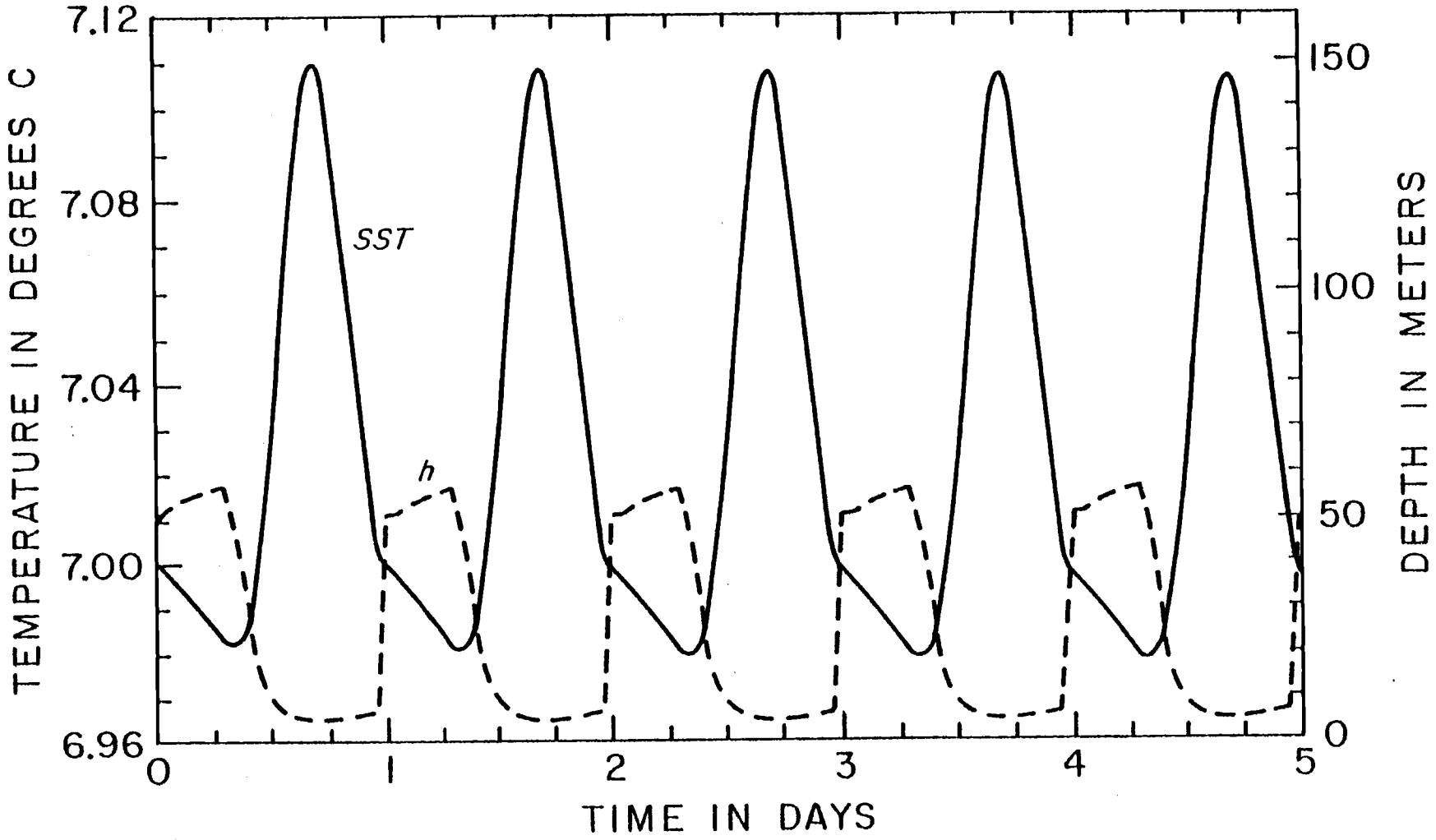

Fig. 21. Time series of SST and h from run D1 using PROG.

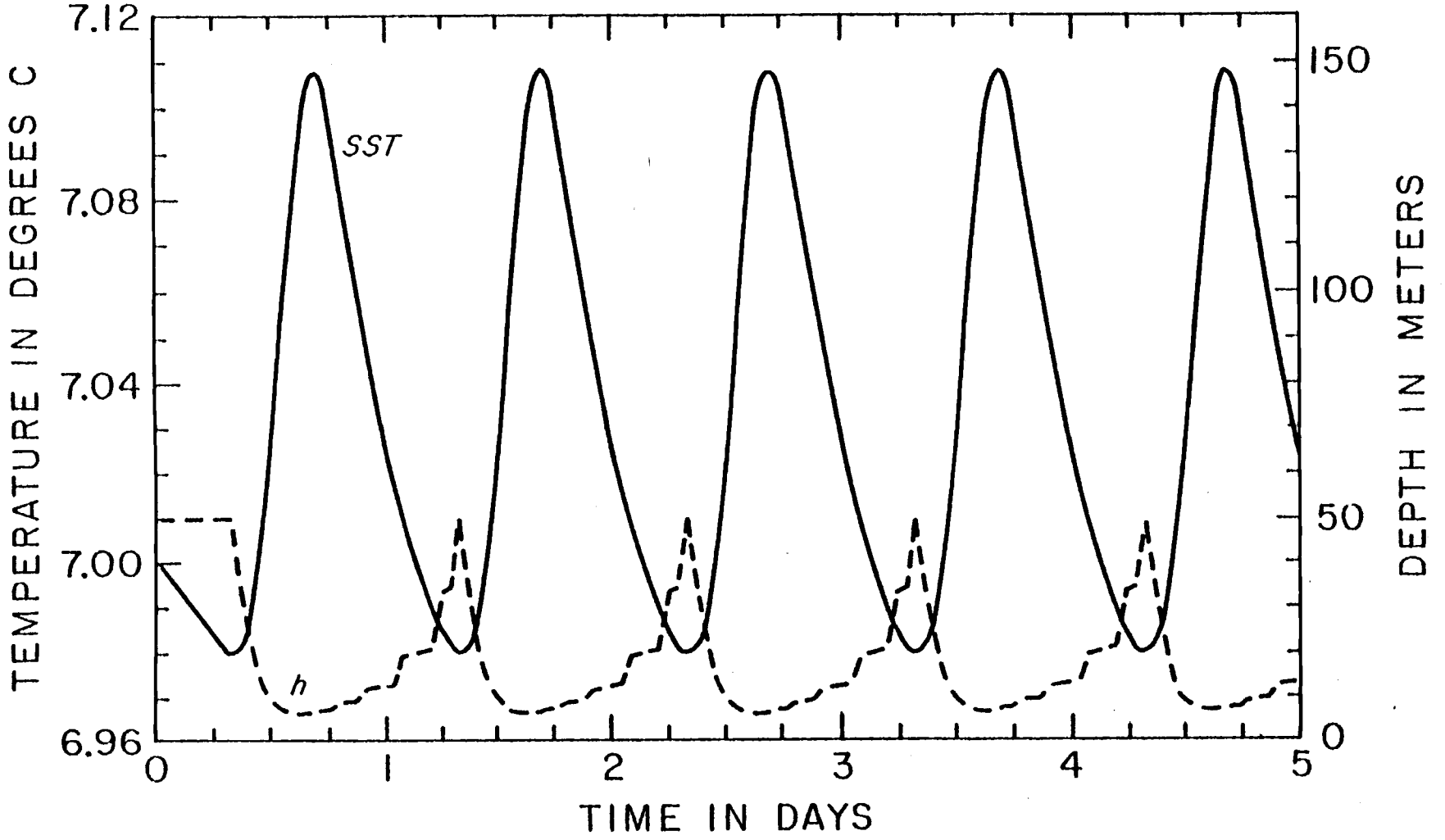

Fig. 22. Time series of SST and h from run D1 using KIM.

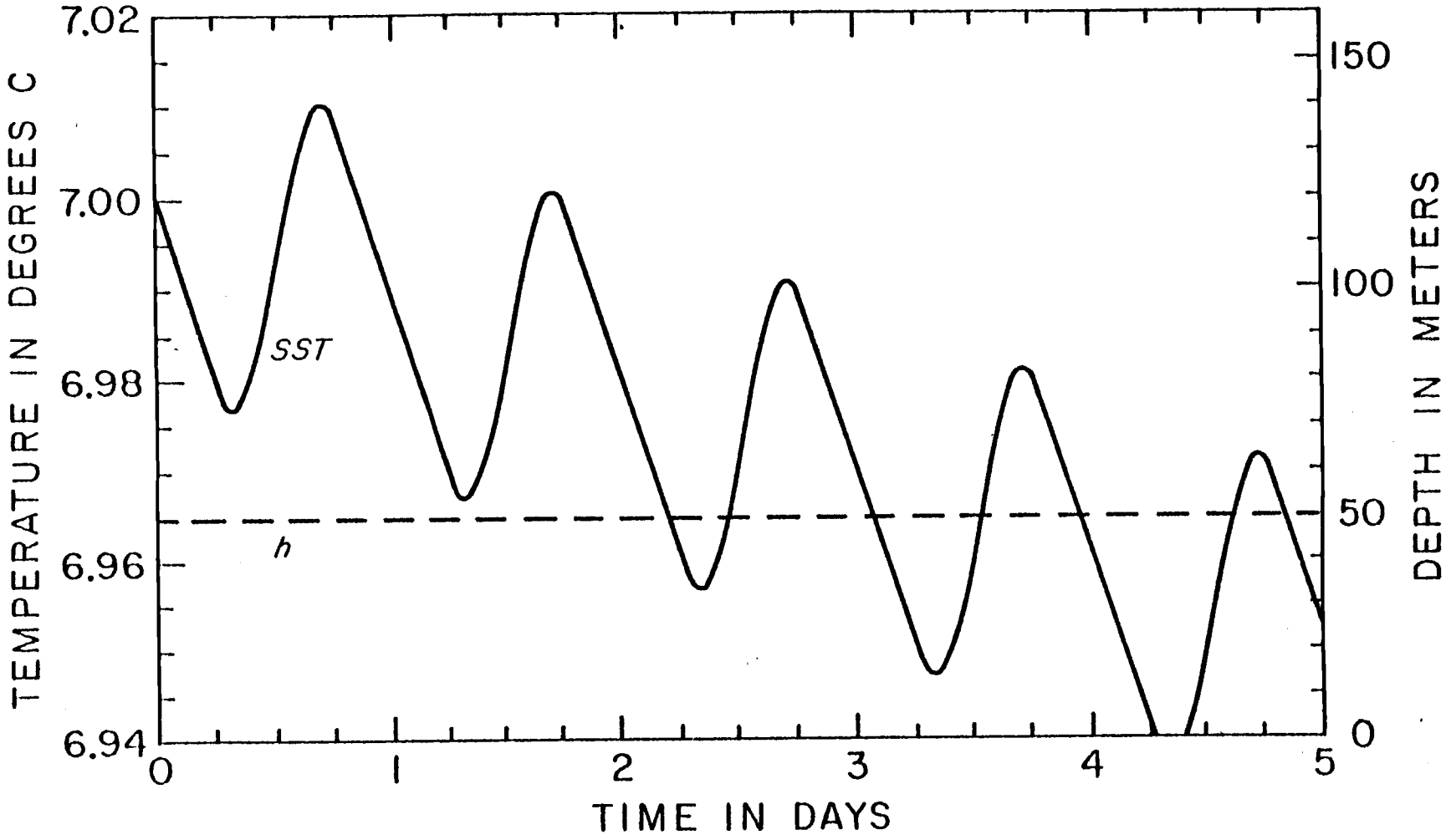

Fig. 23. Time series of SST and h from run D2 using CONS.

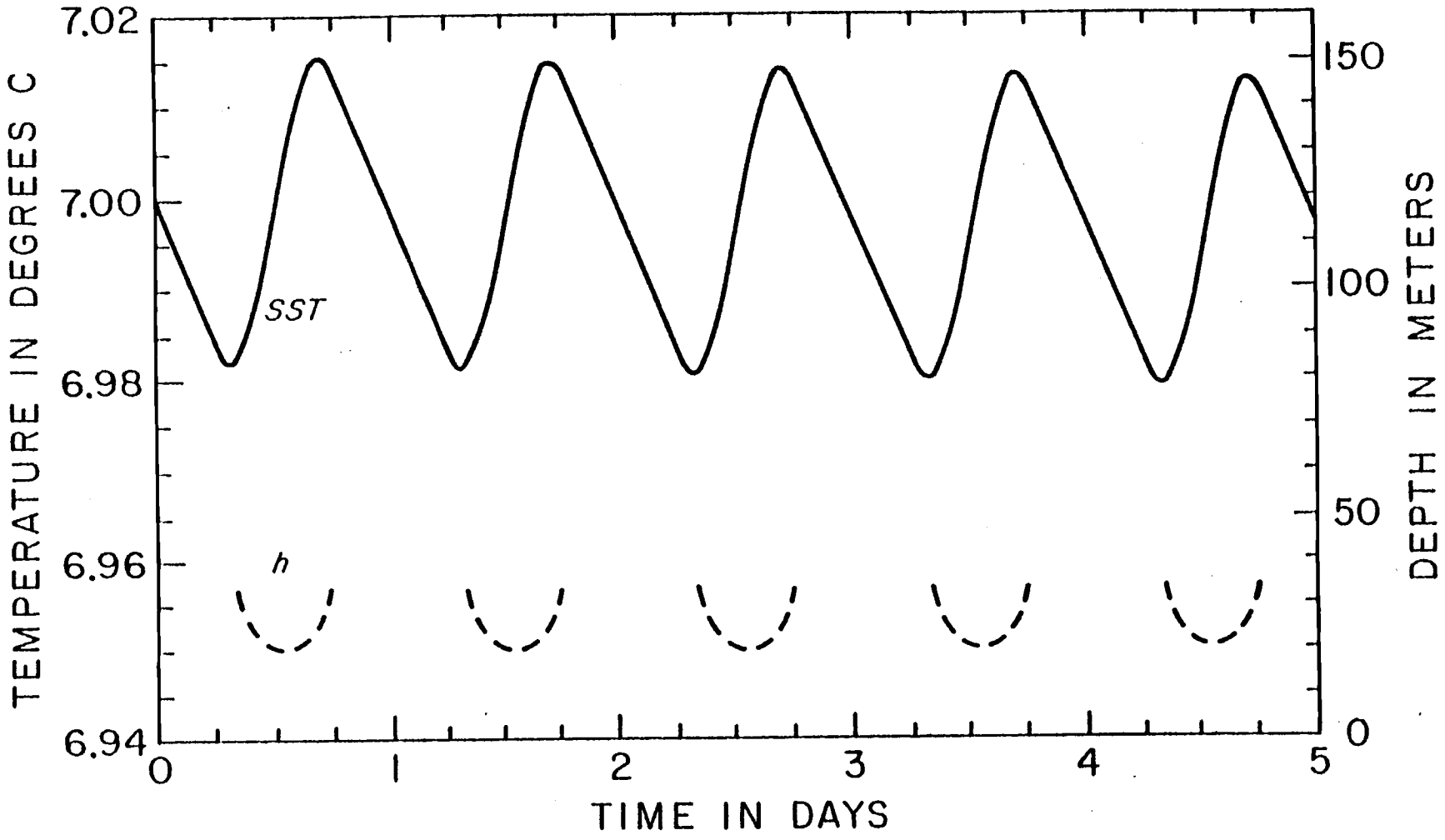

Fig. 24. Time series of SST and h from run D2 using DIAG.

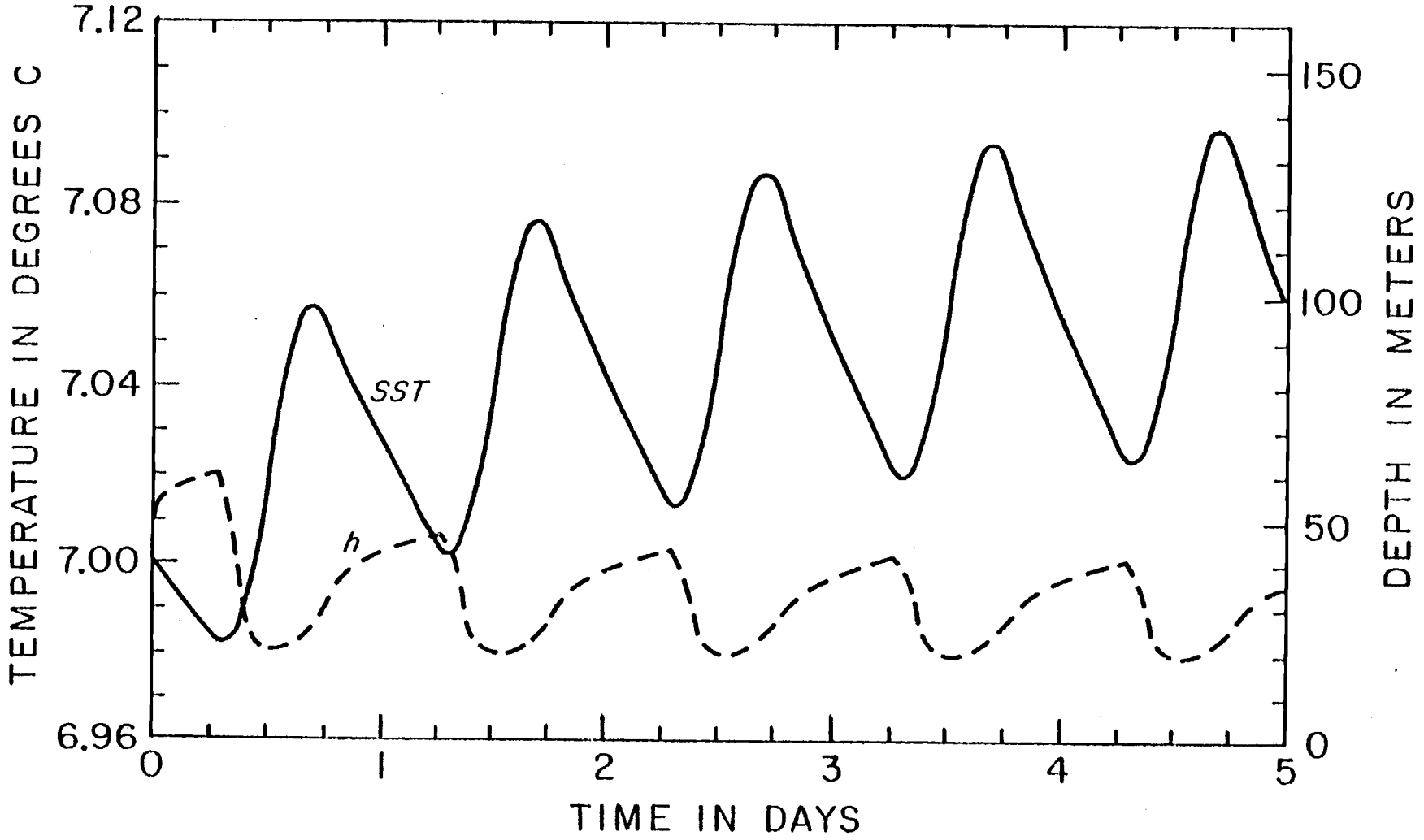

Fig. 25. Time series of SST and h from run D2 using PROG.

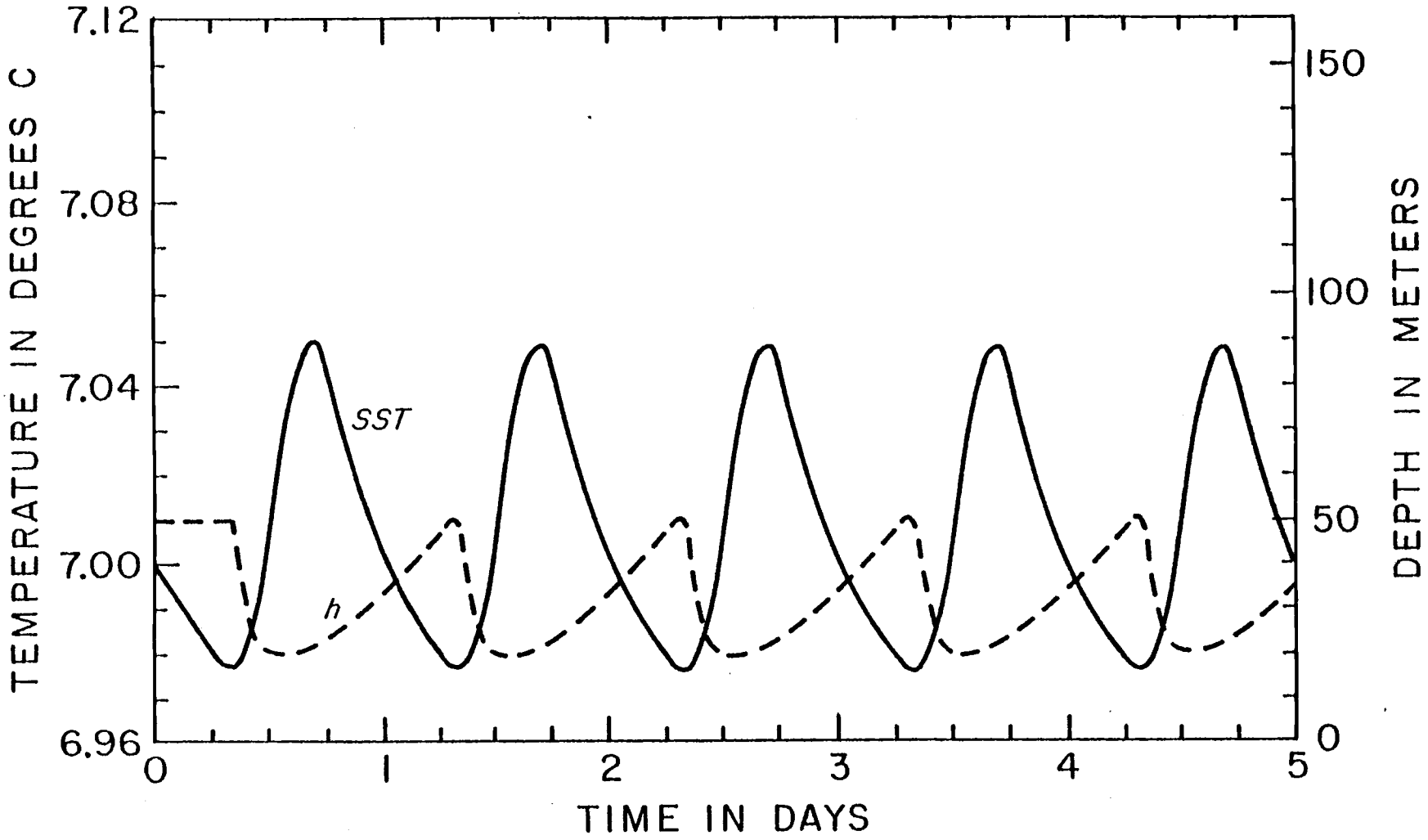

Fig. 26. Time series of SST and h from run D2 using KIM.

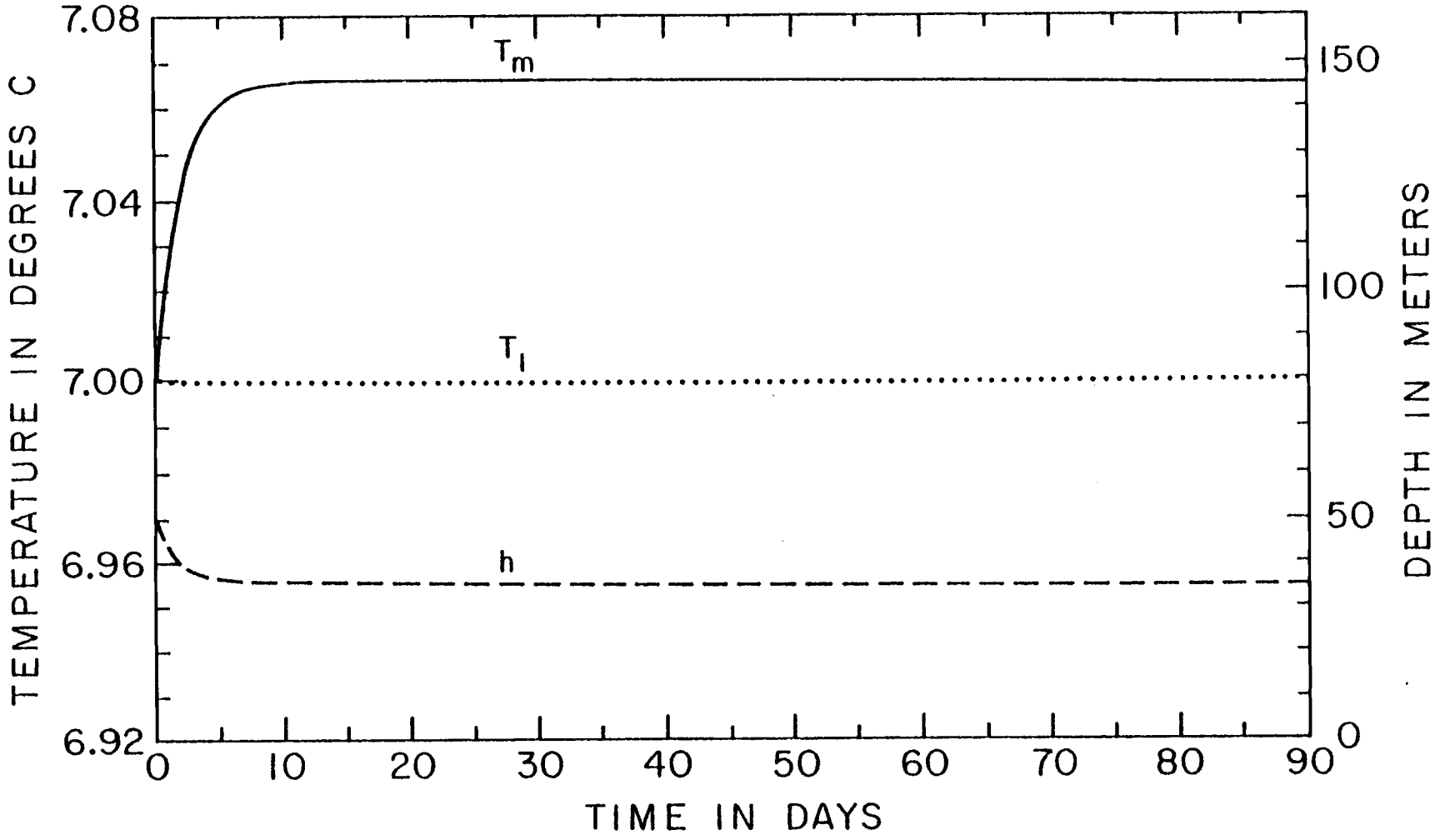

Fig. 27. Ninety day time series of the mixed layer temperature T_m, top OGCM layer temperature T_1, and h at midnight from run D2 using PROG with $\kappa = 0$.

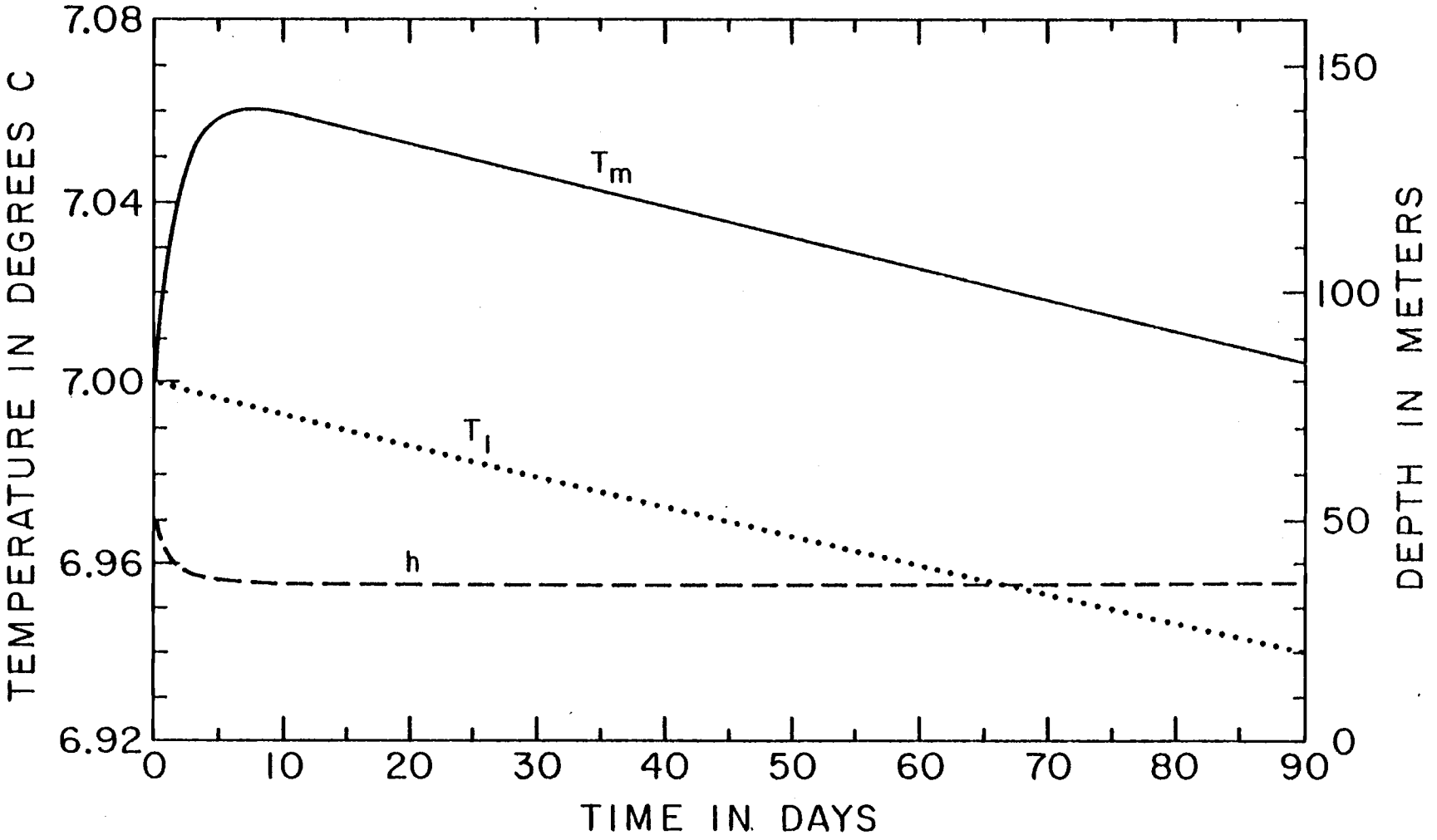

Fig. 28. Ninety day time series of T_m, T_l and h at midnight from run D2 using PROG with κ = .0001 $m^2 s^{-1}$.

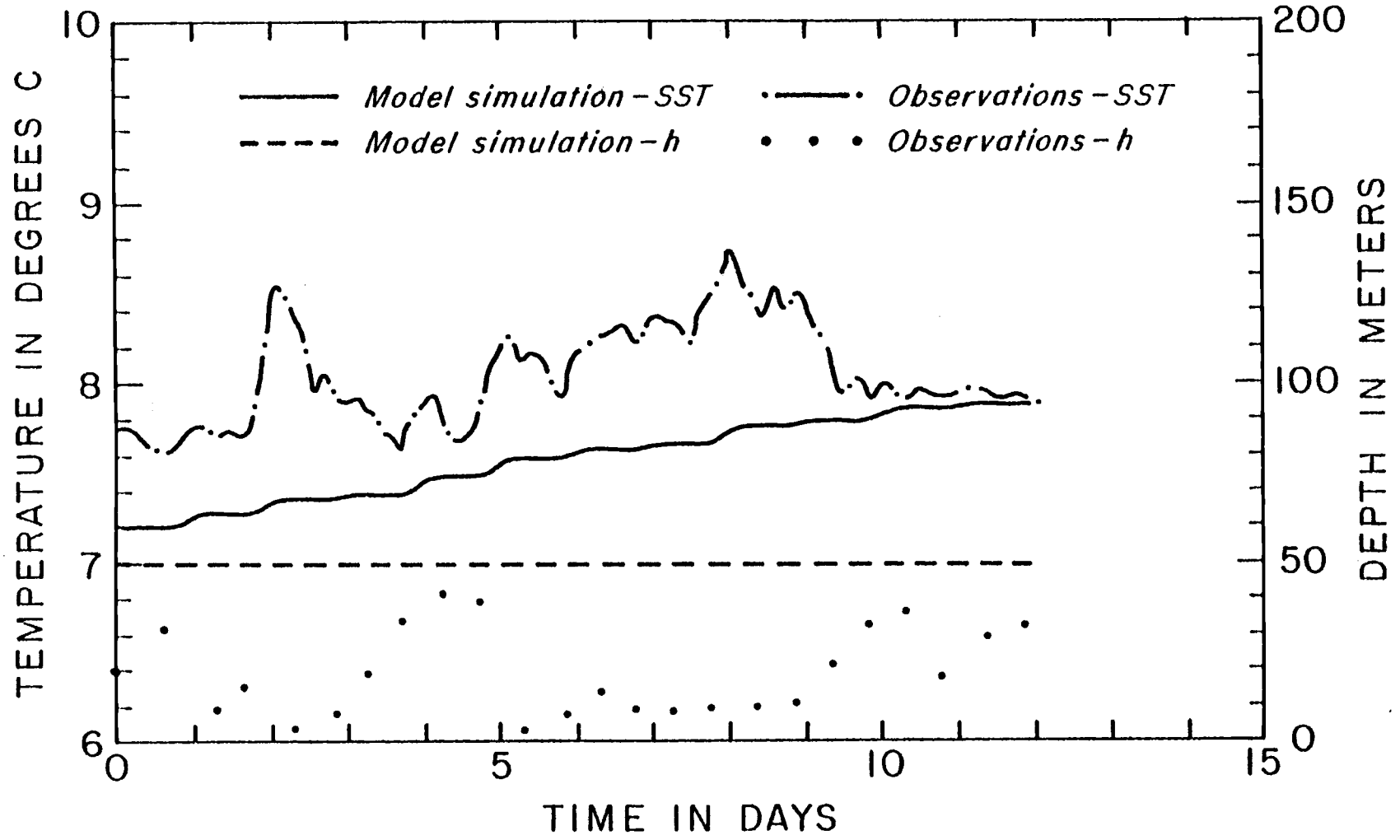

Fig. 29. Time series of SST and h from run DM using DIFF and from observations at Ocean Station PAPA.

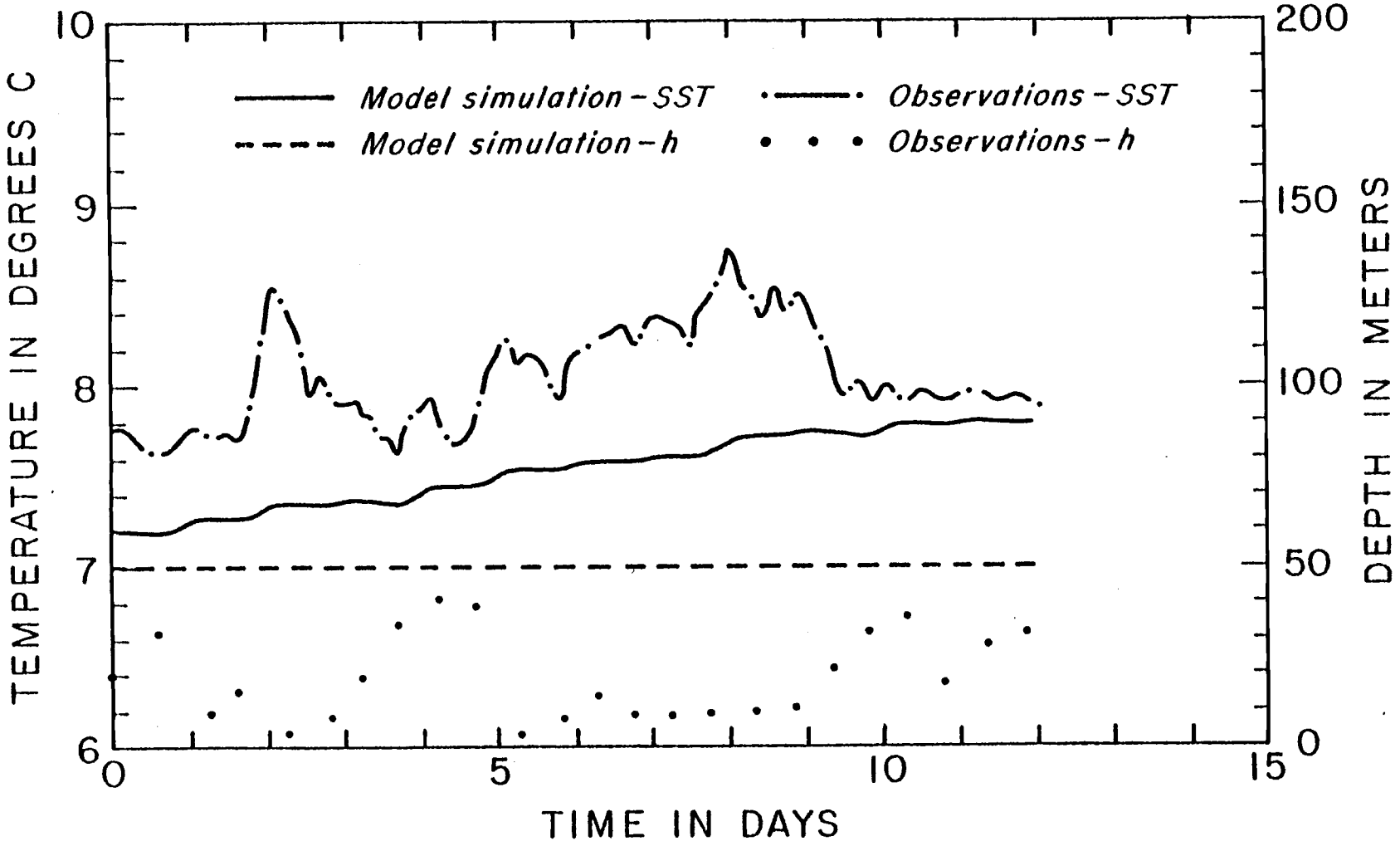

Fig. 30. Time series of SST and h from run DM using CONS and from observation at Ocean Station PAPA.

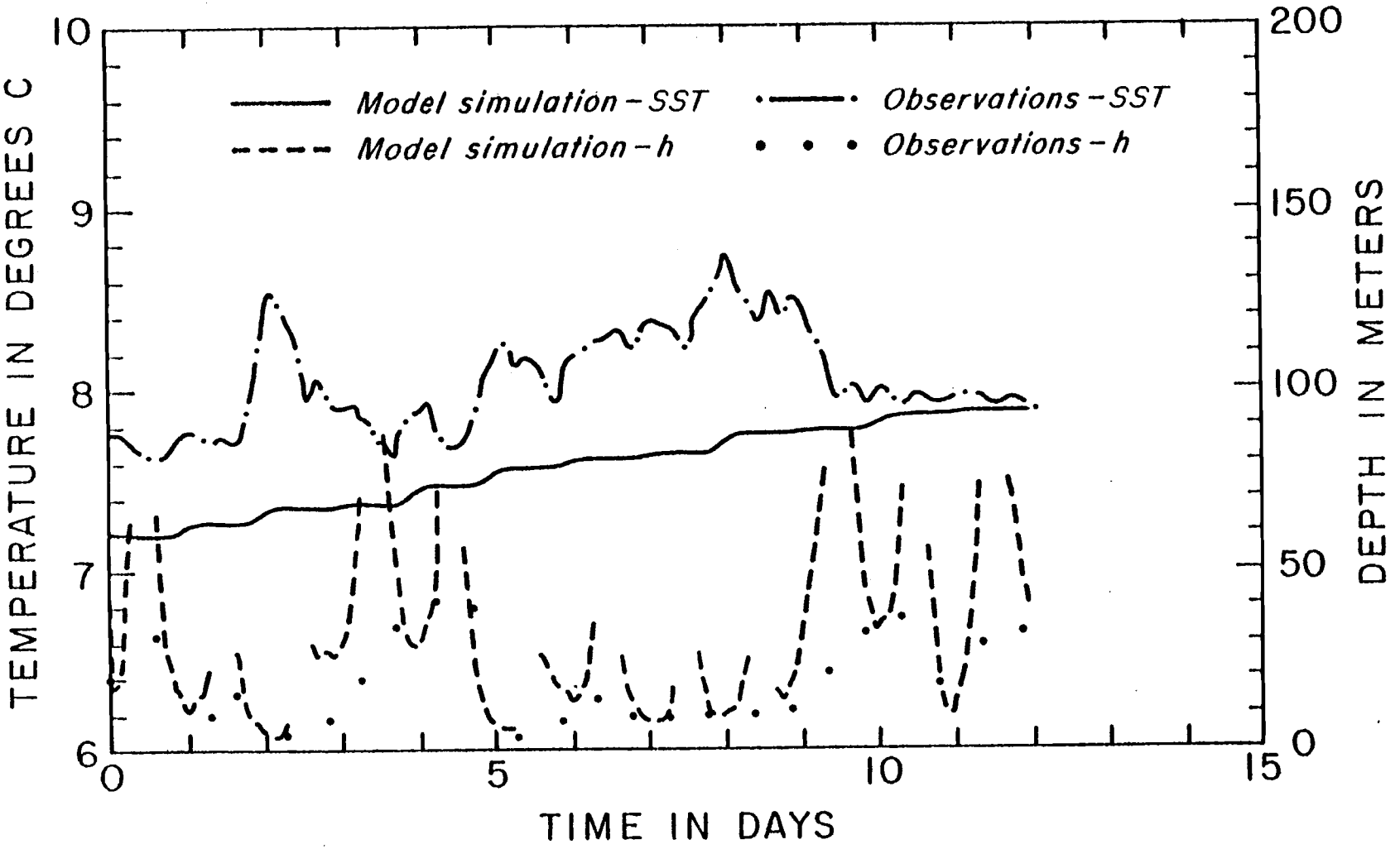

Fig. 31. Time series of SST and h from run DM using DIAG and from observations at Ocean Station PAPA.

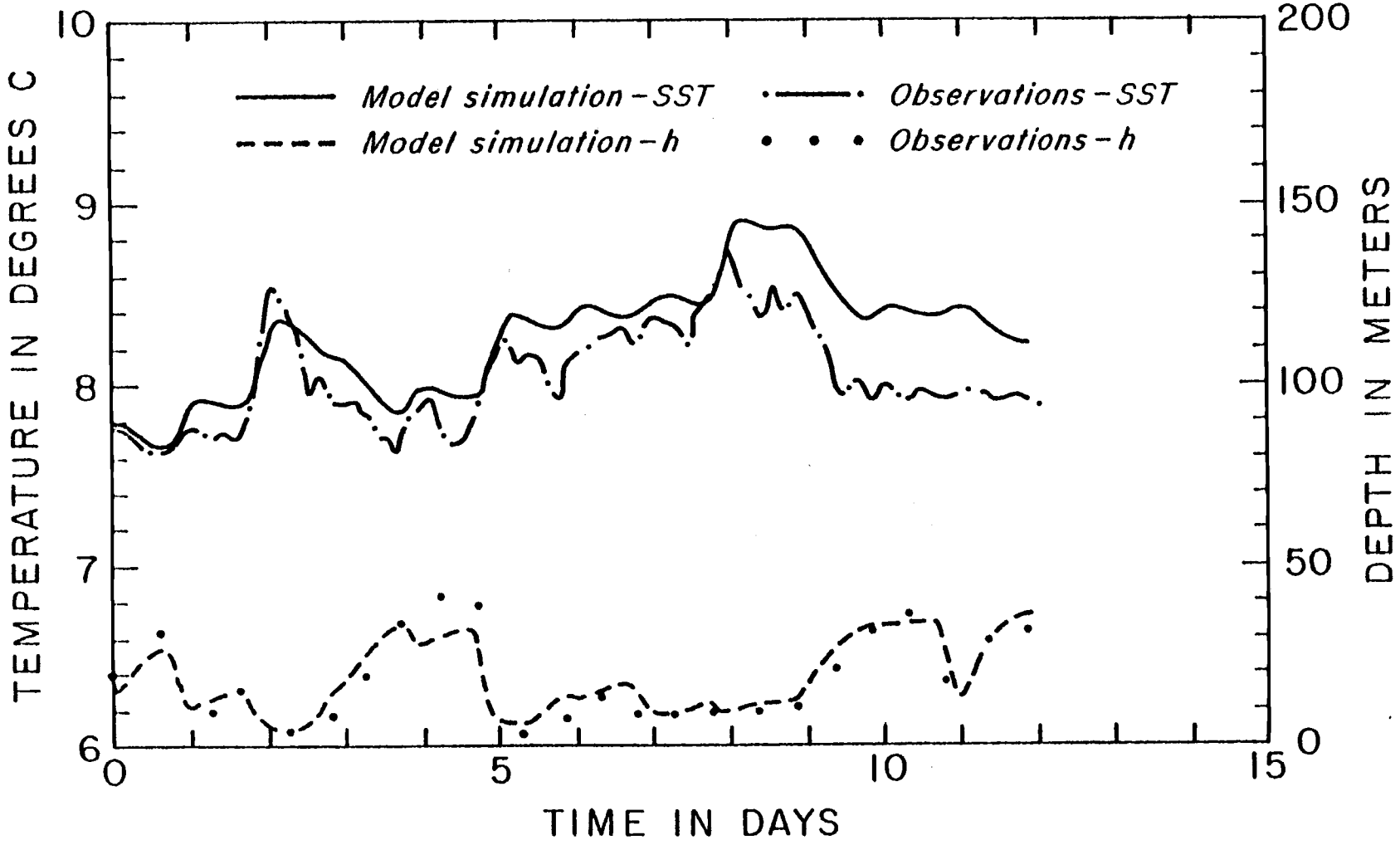

Fig. 32. Time series of SST and h from run DM using PROG and from observations at Ocean Station PAPA.

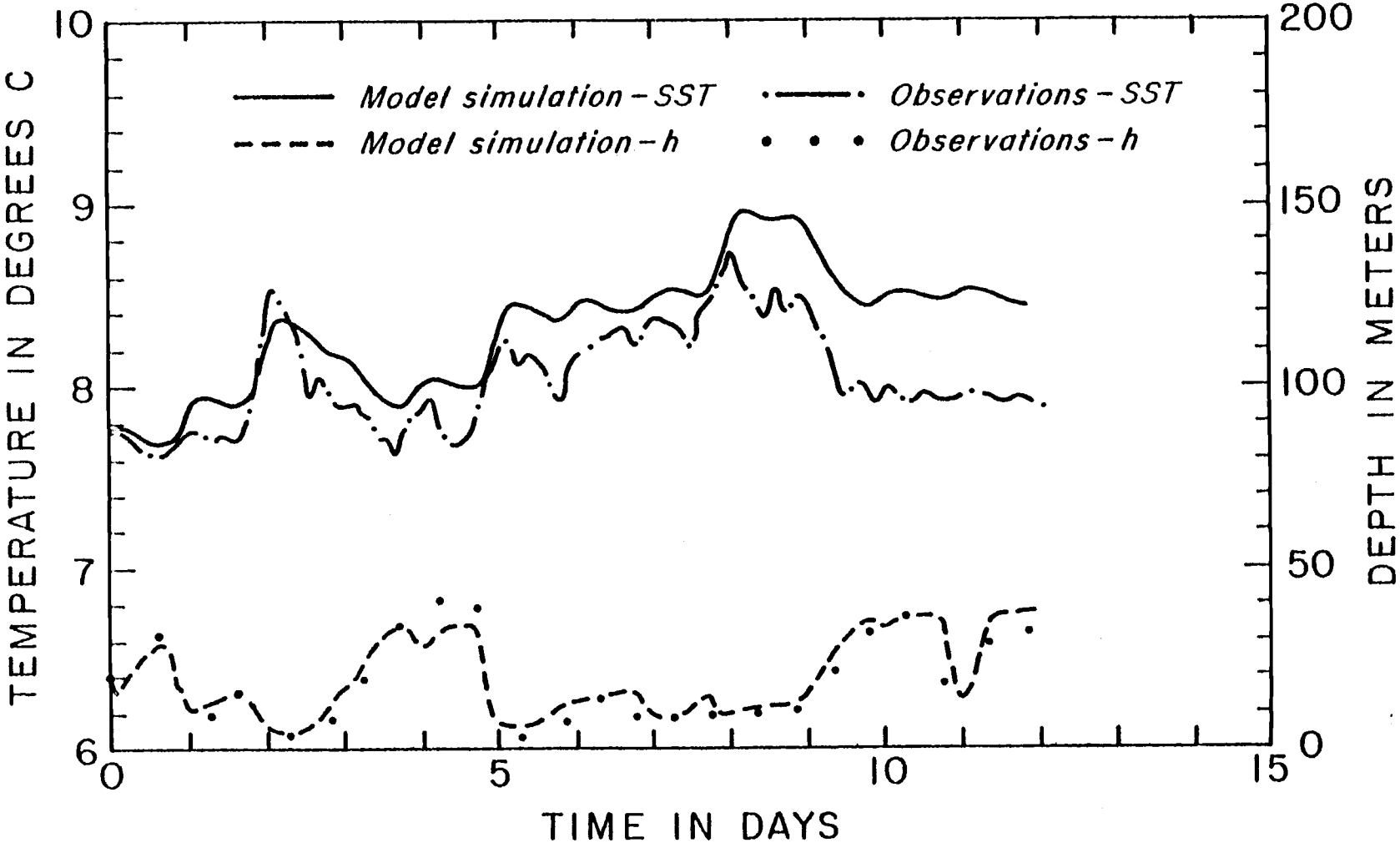

Fig. 33. Time series of SST and h from run DM using KIM and from observations at Ocean Station PAPA.

BIBLIOGRAPHY

Alexander, R.C., and J.-W. Kim, 1976: Diagnostic model study of mixed-layer depths in the summer North Pacific. Journal of Physical Oceanography, 6, 293-298.

Bryan, K., S. Manabe and R.C. Pacanowski, 1975: A global ocean-atmosphere climate model. Part II. The oceanic circulation. Journal of Physical Oceanography, 5, 30-46.

Denman, K.L., 1973: A time-dependent model of the upper ocean. Journal of Physical Oceanography, 3, 173-184.

_____, and M. Miyake, 1973: Upper layer modification of Ocean Station PAPA: observations and simulation. Journal of Physical Oceanography, 3, 185-196.

Dorman, C.E., 1974: Analysis of meteorological and oceanographic data from Ocean Vessel N (30N,140W). Ph.D. Thesis, Oregon State University, Corvallis, Oregon, 136 pp.

Gill, A.E., and J.S. Turner, 1976: A comparison of seasonal thermocline models with observations. Deep-Sea Research, 23, 391-401.

Haney, R.L., and R.W. Davies, 1976: The role of surface mixing in the seasonal variation of the ocean thermal structure. Journal of Physical Oceanography, 6, 504-510.

Kantha, L.H., O.M. Phillips and R.S. Azad, 1977: On turbulent entrainment at a stable density interface. Journal of Fluid Mechanics, 79, 753-768.

Kim, J.-W., 1976: A generalized bulk model of the oceanic mixed layer. Journal of Physical Oceanography, 6, 686-695.

_____, and W.L. Gates, 1978: Simulation of the annual variability of the general circulation of the world ocean (in preparation).

_____, and R.C. Heald, 1978: Parameterization of the oceanic mixed layer for use in general circulation models. Technical Report No. 3, Climatic Research Institute, Oregon State University, Corvallis, Oregon (in preparation).

Kitaigorodsky, S.A., 1960: On the computation of the thickness of the wind-mixing layer in the ocean. Bulletin (Izvestiya) Academy of Sciences, U.S.S.R., Geophysics Series, 3, 284-287.

Kraus, E.B., and C. Rooth, 1961: Temperature and steady state vertical heat flux in the ocean layers. Tellus, 13, 231-238.

_____, and J.S. Turner, 1967: A one-dimensional model of the seasonal thermocline: II. The general theory and its consequences. Tellus, 19, 98-105.

Pollard, R.T., P.B. Rhines and R.O.R.Y. Thompson, 1973: The deepening of the wind-mixed layer. Geophysical Fluid Dynamics, 3, 381-404.

Wyrtki, K., 1965: The average annual heat balance of the North Pacific Ocean and its relation to ocean circulation. Journal of Geophysical Research, 70, 4547-4559.